A Closer Look at TabPFN v2: Understanding Its Strengths and Extending Its Capabilities

Han-Jia Ye & Si-Yang Liu

School of Artificial Intelligence, Nanjing University
National Key Laboratory for Novel Software Technology, Nanjing University
{yehj, liusy}@lamda.nju.edu.cn

Wei-Lun Chao

The Ohio State University chao. 209@osu.edu

Abstract

Tabular datasets are inherently heterogeneous, presenting significant challenges for developing pre-trained foundation models. The recently introduced transformerbased Tabular Prior-data Fitted Network v2 (TabPFN v2) achieves unprecedented in-context learning performance across diverse downstream datasets, marking a pivotal advancement in tabular foundation models. In this paper, we take a closer look at TabPFN v2 to examine how it effectively handles heterogeneity and achieves high predictive accuracy, and to explore how its limitations in high-dimensional, many-category, and large-scale tasks can be mitigated. We find that TabPFN v2 can infer attribute relationships even when provided with randomized attribute token inputs, eliminating the need to explicitly learn dataset-specific attribute embeddings to address heterogeneity. We further show that TabPFN v2 can be transformed into a feature extractor, revealing its ability to construct a highly separable feature space for accurate predictions. Lastly, we demonstrate that TabPFN v2's limitations can be addressed through a test-time divide-and-conquer strategy, enabling scalable inference without requiring re-training. By uncovering the mechanisms behind TabPFN v2's success and introducing strategies to extend its applicability, this study offers key insights into the design of future tabular foundation models.

1 Introduction

Tabular data is ubiquitous across a wide range of applications, including healthcare [32], finance [43], and scientific research [33, 32]. In this format, each instance (e.g., a patient's record) is represented as a vector of attributes, and the goal of a machine learning model is to map these vectors to their corresponding labels [7]. Traditionally, tree-based models [56, 12] have dominated this domain, but recent advances in deep tabular models are increasingly closing the performance gap [22, 29, 76].

However, unlike vision and language domains, where pre-trained foundation models have driven significant progress [40, 81], tabular data is still desperately awaiting a similar breakthrough [63, 27, 54, 82, 77, 66]. A primary challenge arises from the inherent heterogeneity of tabular datasets, which often vary in dimensionality and attribute meanings, making the development of effective and versatile foundation models difficult. Additionally, there is an urgent need for such models, as many tabular datasets are small-scale—such as medical data with limited patient numbers. Training individual models from scratch for these datasets is highly sensitive to hyperparameter choices and often fails to generalize due to limited data [18, 24, 25].

Recently, the Tabular Prior-Fitted Network v2 (TabPFN v2) [28] has emerged as a significant step forward. Built on transformer architectures [67] and pre-trained on gigantic synthetic datasets [27, 28], TabPFN v2 can be directly applied to diverse downstream tasks without additional tuning. Specifically, TabPFN v2 takes both a labeled training set and an unlabeled test instance as input, predicting the test label in an "in-context learning" manner. When evaluated across both classification and regression tasks, TabPFN v2 consistently outperforms prior tabular methods, achieving state-of-the-art accuracy.

Motivated by the remarkable performance of TabPFN v2, we aim to take a step further to understand the mechanisms behind its success ¹—specifically, how it effectively handles dataset heterogeneity and achieves high predictive accuracy. In addition, we investigate how to overcome its current limitations—namely, its suggested data regime of no more than 10,000 samples, 500 dimensions, and 10 classes [28]—ideally without requiring model re-training. We outline major insights as follows.

- 1. **TabPFN v2 internalizes attribute token learning to handle data heterogeneity.** Given an instance with *d* attributes, TabPFN v2 transforms it into a set of fixed-dimensional tokens and uses a transformer architecture to handle variability in *d*, following [64, 22, 74]. In sharp contrast to prior methods that rely on known attribute semantics (*e.g.*, word vectors) or learn dataset-specific attribute tokens, TabPFN v2 instead employs randomized attribute tokens—resampled at each inference. This design "syntactically" allows TabPFN v2 to be directly applied to new downstream datasets with varying dimensionalities and attribute meanings without additional tuning, but raises a fundamental question: how does it still make accurate predictions? Our analysis shows that, regardless of the randomness, TabPFN v2 can consistently infer attribute relationships through in-context learning, essentially integrating attribute token learning into the inference itself. In short, TabPFN v2 unifies representation learning and prediction within a single forward pass.
- 2. **TabPFN v2 can be repurposed as a feature extractor for downstream tasks.** The exceptional predictive performance of TabPFN v2 suggests that it produces instance-level feature representations that are highly discriminative. However, verifying this is non-trivial, as TabPFN v2's in-context learning mechanism assigns distinct roles to labeled training and unlabeled test instances, resulting in embeddings that are not directly comparable. To overcome this, we propose a leave-one-fold-out strategy that enables the extraction of instance features more closely aligned across training and test data. Our findings reveal that TabPFN v2 effectively maps tabular instances into a nearly linearly separable embedding space. Remarkably, training a linear model on these features yields accuracy comparable to that of TabPFN v2's in-context learner, highlighting its potential as a powerful feature encoder. This not only offers insights into TabPFN v2's inner workings but also opens the door to broader applications (*e.g.*, visualization and error analysis).
- 3. **Test-time divide-and-conquer effectively mitigates TabPFN v2's limitations.** As noted in [28], TabPFN v2 faces challenges when applied to high-dimensional, many-category, or large-scale datasets. Rather than resorting to model re-training, we show that these limitations can be effectively addressed through carefully designed *post-hoc* divide-and-conquer strategies, reminiscent of test-time scaling techniques developed for large language models [70, 51]. Empirical results show significant accuracy gains across these challenging data regimes, highlighting the potential of advanced post-hoc methods to further extend the capabilities of tabular foundation models.

Remark. This paper presents a timely and in-depth investigation into TabPFN v2, offering valuable insights for advancing tabular foundation models. While we do not propose a new architecture or training scheme, our contribution lies in the novel analysis and principled extension of TabPFN v2. This reflects a growing trend in foundation model research, where understanding, evaluating, and adapting powerful models is increasingly seen as being as impactful as designing new ones.

2 Related Work

Tabular foundation models. Pre-trained models have revolutionized the vision and language domains [40, 81], but their adoption in tabular data remains limited due to the substantial heterogeneity across datasets. Variations in attribute spaces, dimensionalities, and label distributions present significant challenges for joint training and transferability. One solution is to leverage the semantic meanings of attributes, as demonstrated by methods that convert tabular instances into textual descriptions and

¹We note that TabPFN v2 [28], like many recent large language models (LLMs) and foundation models, does not release its training data or training recipe. Accordingly, our focus is on understanding the properties of the released pre-trained model and exploring ways to extend its applicability.

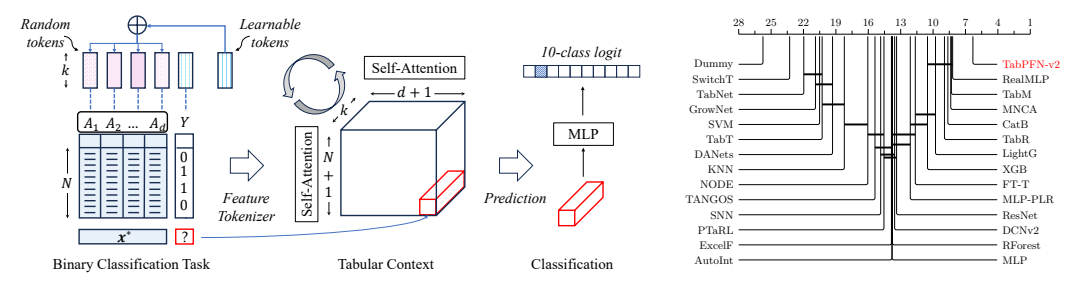


Figure 1: Left: Illustration of TabPFN v2's mechanism for binary classification [28]. $\{A_1,\ldots,A_d\}$ denote d attributes of the task. Training examples and a test instance are combined into a tabular context and transformed into a $(N+1)\times(d+1)\times k$ tensor using a combination of learnable and randomized tokens. Two types of self-attention are applied alternately across rows (inter-sample) and columns (inter-feature). The output token corresponding to the (dummy) label of the test instance is processed through an MLP to generate a 10-class logit. Right: Wilcoxon-Holm test at a significance level of 0.05 over 273 small- to medium-scale datasets. We omit the 27 datasets used to select TabPFN v2's checkpoint from the 300 datasets in [75].

apply large language models for prediction [26, 79, 69, 71]. Alternatively, some approaches aim to improve transferability by pre-computing attribute tokens based on semantic embeddings [74, 39]. In practical domains such as healthcare or scientific measurement, the semantic meanings of attributes are often inaccessible due to privacy constraints, annotation costs, or a lack of describability. To address this, [77] proposed representing each instance by its similarity profile to a fixed number of nearest neighbor examples, thereby mapping it into a consistent latent space with shared dimensional semantics. The TabPFN family [27, 28] leverages the in-context learning capabilities of transformers to directly predict labels by contextualizing test instances among training examples. This strategy inspired subsequent pre-trained tabular models such as [48, 15, 57]. While TabPFN v1 pads attribute vectors to a fixed dimension, TabPFN v2 introduces a specialized attribute tokenizer to handle heterogeneous input spaces. Meta-learning has also been explored to generate model weights tailored for downstream tabular tasks with limited data [34, 6, 50]. Other pre-trained models rely on lightweight fine-tuning to adapt to variations in attribute and label spaces [44, 80, 62, 82].

3 Background

Learning with a single tabular dataset. A tabular dataset $\mathcal{D} = \{(x_i, y_i)\}_{i=1}^N$ contains N training examples, corresponding to the rows in a table. Each instance x_i is characterized by d features or attributes (*i.e.*, columns in the table), where d typically varies across datasets. Its label y_i belongs to $[C] = \{1, \ldots, C\}$ for a classification task or is a numerical value for a regression task. We assume that all attributes of an instance are numerical (continuous). Categorical (discrete) attributes, if present, are transformed using ordinal or one-hot encoding beforehand. The goal of tabular machine learning is to learn a mapping f from instances to their labels. Specifically, given an unseen instance $x^* \in \mathbb{R}^d$ sampled from the same distribution as \mathcal{D} , the learned mapping f predicts its label as $\hat{y}^* = f(x^* \mid \mathcal{D})$. A smaller discrepancy between \hat{y}^* and the true label y^* indicates stronger generalizability of f.

TabPFN. The original TabPFN implements f for classification using a transformer-like architecture [27]. Both training and test instances are first zero-padded to a fixed dimension k' (e.g., 100). Then, x_i and y_i are linearly projected to $\tilde{x}_i \in \mathbb{R}^k$ and $\tilde{y}_i \in \mathbb{R}^k$, respectively. TabPFN processes both a labeled training set and an unlabeled test instance jointly, predicting the test label in an in-context learning manner. The task context is defined as $\mathcal{C} = \{(\tilde{x}_1 + \tilde{y}_1), \dots, (\tilde{x}_N + \tilde{y}_N), (\tilde{x}^*)\} \in \mathbb{R}^{(N+1)\times k}$, consisting of N+1 tokens, each of dimension k. These tokens are processed by multiple transformer layers, which accommodate variable-length inputs (i.e., variable N). The output token corresponding to the test instance is passed through a multi-layer perceptron (MLP) to produce a 10-class logit.

TabPFN v2. The recently proposed variant [28] introduces several key modifications. First, each of the d attributes in \mathcal{D} is embedded into a k-dimensional space, with random perturbations added to differentiate attributes. Together with the label embedding $\tilde{y}_i \in \mathbb{R}^k$, each training instance x_i is represented by (d+1) tokens with dimension k. For a test instance x^* , where the label is unknown, a dummy label (e,g), the average label of the training set) is used to generate the label embedding \tilde{y}^* .

The full input to TabPFN v2—comprising the training set and the test instance—is thus represented as a tensor of shape $(N+1) \times (d+1) \times k$. Two types of self-attention are applied in alternation: one over samples (among the N+1 instances) and the other over attributes (among the d+1 dimensions),

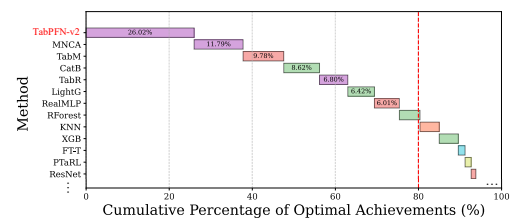


Figure 2: Probability of Achieving the Maximum Accuracy or Minimum RMSE across 273 datasets. Values inside rectangles show the percentage of datasets on which a method achieves the best result.

| + | TabPFN v2 | CatB | MNCA | R-MLP | LR |
|-------------|-----------|------|------|-------|------|
| High-Dim | 3.36 | 2.82 | 4.41 | 2.14 | 2.27 |
| Large-Scale | 3.97 | 1.89 | 2.27 | 1.94 | 4.47 |
| >10 classes | 3.33 | 2.75 | 3.17 | 1.42 | 4.33 |

Table 1: Average rank (lower is better) of TabPFN v2 and representative baselines on 18 high-dimensional, 18 large-scale, and 12 datasets with more than 10 classes. Full results with our extensions are in Figure 5.

enabling in-context learning along both axes. Finally, the output token corresponding to the test instance's dummy label \tilde{y}^* is extracted and mapped to a 10-class logit for classification or a single-value logit for regression. An overview of this process is illustrated in Figure 1 (left).

The weights in TabPFN v2 are pre-trained on diverse synthetic datasets generated using structural causal models (SCMs), with the checkpoint selected based on real-world datasets. For additional details, including feature pre-processing, acceleration, and post-hoc ensembling, please refer to [28].

Remark. In the tabular domain, years of research into deep and foundation models have culminated in TabPFN v2 [28]—a breakthrough that, for the first time, enables deep models to consistently outperform traditional methods without fine-tuning. However, due to venue constraints, many technical details were omitted from the main paper. For example, the use of randomized tokens was documented in the supplementary material and code. In light of this, we aim to systematically analyze TabPFN v2, as we believe such a study is more impactful than proposing yet another architecture.

4 Comprehensive Evaluation of TabPFN v2

Before presenting our core studies, we first extend TabPFN v2's evaluation beyond the original set of datasets to over 300, covering a much broader range of domains, attributes, scales, dimensionalities, and tasks [23, 49, 75, 60], aiming to more thoroughly assess its generalizability and limitations.

4.1 Setups

We first adopt the benchmark from [75], comprising 120 binary classification, 80 multi-class classification, and 100 regression tasks. It resolves common issues such as mislabeled data and redundancies from overlapping dataset versions [42], enabling more reliable evaluations. Out of the 300 datasets, 27 belong to the validation set used for checkpoint selection in TabPFN v2 [28]. To avoid evaluation bias, we exclude these datasets and report results on the remaining 273 datasets.

Following the protocol in [21, 22], each dataset is randomly split into training, validation, and test partitions in a 64%/16%/20% ratio. TabPFN v2 predicts test set labels directly using in-context learning, without any additional parameter or hyperparameter tuning. Baseline tabular methods—both deep and traditional—perform hyperparameter tuning using Optuna [1], with 100 trials on the training set and early stopping based on validation performance.

All methods are evaluated using 15 random seeds, and we report the average performance across seeds. For classification tasks, we report accuracy (higher is better), while regression tasks are evaluated using Root Mean Square Error (RMSE; lower is better). For tasks with more than 10 classes, we adopt the built-in Error-Correcting Output Codes (ECOC) strategy for TabPFN v2.

4.2 Empirical Results: Strengths of TabPFN v2

We compare TabPFN v2 against 26 representative tabular methods (see Appendix for full references). To assess statistical significance, we apply the Wilcoxon-Holm test with a significance level of 0.05 [14]. As shown in the critical difference diagram in Figure 1 (right), TabPFN v2 consistently outperforms both tree-based methods, such as CatBoost [56], and deep tabular models, including RealMLP [29], ModernNCA [76], TabM [19], TabR [21], and FT-Transformer [22].

To further assess performance, we report the Probability of Achieving the Maximum Accuracy or Minimum RMSE (PAMA) [13], which measures the proportion of datasets on which a method achieves the best performance. As shown in Figure 2, TabPFN v2 attains the highest score, delivering the top results on 26.02% of the datasets—outperforming other methods such as ModernNCA (11.79%) and TabM (9.78%). These results underscore TabPFN v2's strong generalizability.

4.3 Empirical Results: Limitations of TabPFN v2

The above evaluation focuses on small- to medium-scale datasets, specifically those with fewer than 10,000 examples. However, as noted in [28], the computational complexity of transformers constrains TabPFN v2's ability to scale effectively to datasets with larger sample sizes or higher dimensionality.

To verify this, we conduct additional evaluations on 18 high-dimensional datasets with $d \geq 2,000$ [36] and 18 large-scale datasets where $N \times d > 1,000,000$. For high-dimensional datasets, we follow the same protocol as before. For large-scale datasets, due to the prohibitive cost of hyperparameter tuning, default hyperparameters are used for all methods. The average ranks of several representative methods are summarized in Table 1. The full results—along with our extensions—are in Section 7.

As shown, TabPFN v2's performance degrades on both large-scale and high-dimensional datasets. On large-scale datasets, it ranks below both CatBoost and RealMLP; on high-dimensional datasets, it even falls behind the simple Logistic Regression (LR) model. Beyond these two limitations, Table 1 also reports results on the 12 datasets in Section 4.2 that contain more than 10 categories, where the ECOC strategy currently used by TabPFN v2 appears ineffective in achieving high accuracy. While increased computational complexity may contribute to this reduced effectiveness, we hypothesize that TabPFN v2 was pre-trained exclusively on small- to medium-scale synthetic datasets with fewer than 10 categories, leading to a mismatch when applied to larger or more complex real-world data.

These results underscore the limitations of TabPFN v2, suggesting areas for further improvement.

5 How Does TabPFN v2 Effectively Handle Data Heterogeneity?

Section 4 demonstrates TabPFN v2's excellent generalizability to heterogeneous downstream tasks while also highlighting its current limitations. In the rest of the paper, we first examine the mechanisms behind its strengths, followed by methods to overcome its limitations.

5.1 Diving into TabPFN v2's Mechanisms for Heterogeneous Input

Revisiting the problem. As noted in Sections 2 and 3, tabular datasets often differ in both the number of attributes (i.e., d) and the semantics of those attributes. Even when dimensionalities match, the dimensional semantics from different datasets are typically not directly comparable. A robust tabular foundation model must therefore handle such heterogeneity effectively, enabling it to learn from diverse pre-training datasets and transfer its capabilities to new downstream tasks.

Tokenization as a feasible solution. Among prior approaches, the most relevant to TabPFN v2 are token-based methods [64, 22, 74]. The core idea is to convert a d-dimensional instance $\boldsymbol{x} \in \mathbb{R}^d$ into a set of d fixed-dimensional tokens (each of dimension k), with one token per attribute. This enables the use of transformer architectures, which naturally accommodate variability in d across datasets.

To embed each attribute into a shared k-dimensional space, prior work either uses pre-defined semantic embeddings [74] (e.g., word vectors of attribute names) or learns dataset-specific embeddings [64, 22]. Given d attribute-specific tokens $[\boldsymbol{r}_1,\ldots,\boldsymbol{r}_d]\in\mathbb{R}^{d\times k}$, each instance $\boldsymbol{x}_i\in\mathbb{R}^d$ can then be transformed into $\left[x_i^1\cdot\boldsymbol{r}_1,\ldots,x_i^d\cdot\boldsymbol{r}_d\right]\in\mathbb{R}^{d\times k}$, where x_i^j denotes the j-th element of \boldsymbol{x}_i .

By embedding all attributes into a shared, fixed-dimensional feature space, this approach allows the transformer to learn transferable patterns and knowledge from heterogeneous datasets.

Difficulty in direct generalization. While appealing, the aforementioned methods face a notable challenge when applied to downstream tasks: attribute names or semantics are not always accessible, as discussed in Section 2. Although it is possible to learn dataset-specific attribute tokens, doing so incurs additional computational cost and prohibits the reuse of previously learned tokens. Consequently, this limits the direct generalization of the foundation model to new tasks.

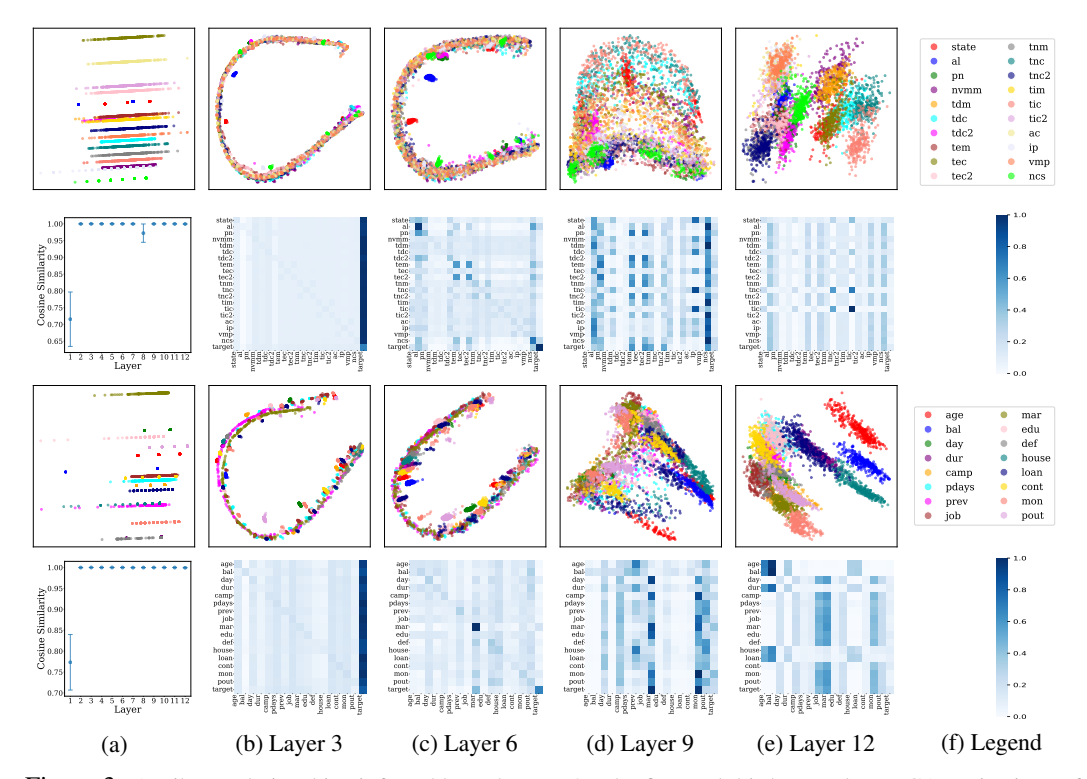


Figure 3: Attribute relationships inferred by TabPFN v2. The first and third rows show PCA projections of the d attribute tokens from all N training instances at various layers for the *churn* and *bank* datasets. Colors indicate different attributes (see legend on the right). The second and fourth rows display the attribute-wise attention maps. Each matrix cell represents the average attention weight between attributes; *the last element along each axis* (e.g., *the last column and row*) *corresponds to the label*. The first plots in the second and fourth rows summarize the cosine similarity of attention maps across random seeds. See text for details.

TabPFN v2's mechanisms. TabPFN v2 builds on prior token-based methods by representing each instance \boldsymbol{x}_i as a sequence of tokens. However, rather than assigning a deterministic token to each attribute, TabPFN v2 samples random tokens at inference time. Specifically, it learns a shared vector $\boldsymbol{u} \in \mathbb{R}^k$ that lifts each element of \boldsymbol{x}_i into a k-dimensional space. To distinguish attributes, TabPFN v2 adds a random perturbation to each one. For the j-th attribute (i.e., x_i^j), the representation becomes $x_i^j \cdot \boldsymbol{u} + \boldsymbol{r}_j$, where $\boldsymbol{r}_j = \boldsymbol{W} \boldsymbol{p}_j$. Here, $\boldsymbol{p}_j \in \mathbb{R}^{k'}$ is a randomly generated vector, and $\boldsymbol{W} \in \mathbb{R}^{k \times k'}$ is a learned projection matrix that conditions the perturbation. The full instance \boldsymbol{x}_i is then represented as:

$$[x_i^1 \cdot \boldsymbol{u} + \boldsymbol{r}_1, \dots, x_i^d \cdot \boldsymbol{u} + \boldsymbol{r}_d, \tilde{\boldsymbol{y}}_i] \in \mathbb{R}^{k \times (d+1)}, \tag{1}$$

where the last token \tilde{y}_i encodes the label information (see Figure 1 for an illustration).

5.2 TabPFN v2 Internalizes Attribute Token Learning

TabPFN v2's randomized tokenization scheme eliminates the need to define attribute- or dataset-specific tokens across tasks, thereby *syntactically* enabling direct application of the pre-trained model. At first glance, this may appear to disregard the valuable *semantic* meaning of attributes. However, we show that through in-context learning, TabPFN v2 can consistently infer relationships among attributes within a dataset—despite the randomness introduced during tokenization. Specifically, we analyze the behavior of attribute tokens from three perspectives, as illustrated in Figure 3, using two representative downstream datasets: *churn* and *bank*.

First, we visualize the attribute token embeddings (i.e., the first d tokens in Equation (1)) across all N training instances. The first and third rows of Figure 3 present PCA projections of these $N \times d$ tokens at the input stage and after transformer layers $\{3,6,9,12\}$, with colors indicating different attributes. Initially, tokens from different attributes appear randomly scattered. However, as the input progresses through the transformer layers, these tokens become increasingly structured. For example,

²This detail was identified from the supplementary material and code of [28].

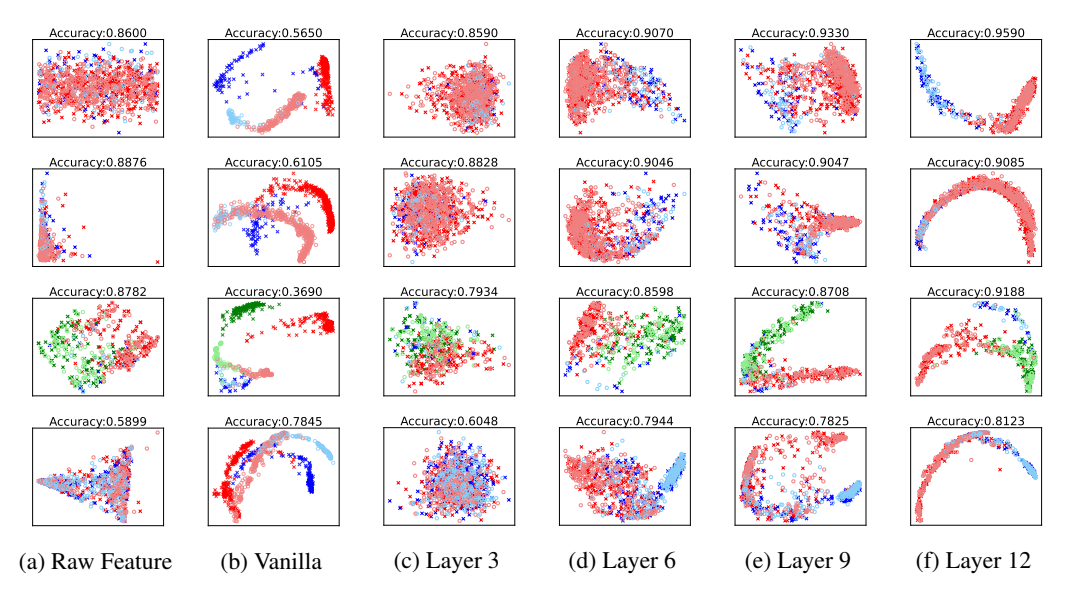


Figure 4: Visualization of the extracted instance features from four datasets: churn (first row, binary), bank (second row, binary), $website_phishing$ (third row, three classes), and KDD (fourth row, binary). Blue and red indicate classes; darker crosses and lighter circles denote training and test samples. (a) shows the raw input features $(e.g., x_i)$, while (b) presents embeddings from the vanilla strategy. (c)-(f) display embeddings produced by our method at different layers. Classification accuracy is reported by training a linear logistic regression model on the training embeddings and evaluating on the test set.

in the *bank* dataset (which predicts term deposit subscriptions), attributes such as "job," "education," and "balance" eventually cluster into semantically coherent groups.

Second, we examine attribute-wise attention patterns across layers, including attention to the label token. The second and fourth rows of Figure 3 show heatmaps of attention weights averaged over heads and training instances. Each row in the heatmap represents the attention distribution from one attribute to all others; the last element along each axis (e.g., the last column and row) corresponds to the label. Darker shades indicate stronger attention. We observe a consistent pattern across datasets: in early layers, attributes predominantly attend to the label token, likely to absorb task-specific signals. In intermediate layers, attention becomes more uniformly distributed, facilitating information exchange across attributes. In deeper layers, attention concentrates on semantically relevant attributes, suggesting the model has inferred inter-attribute relationships useful for prediction.

Lastly, to assess robustness against random token initialization, we compute attribute-wise attention weights across 10 runs. The cosine similarities and variances of these attention patterns are summarized in the first plots of the second and fourth rows in Figure 3. The results confirm that attention patterns remain stable across runs, except for the first layer.

Remark. The above results suggest that TabPFN v2 can reliably infer meaningful attribute relationships through in-context learning. Although input embeddings are randomized, they consistently differentiate attributes across instances—functionally akin to one-hot encodings. Pre-training on diverse tasks thus enables the model to extract predictive patterns (*e.g.*, co-occurrence across attributes, value distributions, and relative magnitudes) directly from the statistical structure of each dataset, without relying on pre-defined attribute semantics. As a result, the model effectively internalizes attribute token learning within the inference process. See the Appendix for further discussion.

6 TabPFN v2 Can Be Transformed into an Effective Feature Encoder

In Section 5, we show that TabPFN v2's in-context learning process infers meaningful attribute relationships. Here, we examine whether TabPFN v2 also produces separable instance representations.

6.1 Naive Feature Extraction Fails

As shown in Figure 1 (left), TabPFN v2 makes predictions based on the output token corresponding to the (dummy) label embedding \tilde{y}^* of the test instance. This output token can thus be interpreted as the

instance embedding for the test example. A natural extension to obtain embeddings for the training instances is to extract the output tokens corresponding to the training label embeddings $\{\tilde{y}_i\}_{i=1}^N$.

However, as shown in Figure 4 (b), this naive approach leads to surprisingly discrepant feature distributions between training (darker cross) and test (lighter circle) examples. As a result, a linear classifier trained on these embeddings performs poorly on the test set. We attribute this discrepancy to the distinct roles of labeled training data and unlabeled test data in TabPFN v2's in-context learning process. Specifically, the label embeddings for the training instances are derived from true labels, whereas those for the test instances rely on dummy labels. This mismatch renders the resulting output embeddings *non-comparable* between training and test instances.

6.2 Leave-one-fold-out Feature Extraction

To address this challenge, we propose a leave-one-fold-out strategy that enables the extraction of comparable embeddings for training and test data. In the TabPFN v2 framework, we treat examples with true labels as the support set \mathcal{S} , and those with dummy labels as the query set \mathcal{Q} . Under the standard configuration, \mathcal{S} corresponds to the labeled training set and \mathcal{Q} to the unlabeled test instances. To extract comparable embeddings for the training examples, they must also be included in \mathcal{Q} with dummy label embeddings. This, however, creates a dilemma: effective in-context learning relies on maximizing the size of \mathcal{S} to ensure sufficient knowledge transfer to \mathcal{Q} . Including training examples in \mathcal{Q} thus competes with the need to keep \mathcal{S} as large as possible.

To overcome this dilemma, we partition the training set into multiple folds (e.g., 10). In each round, one fold serves as Q—with dummy labels used for embedding extraction—while the remaining folds form S with true labels. This setup preserves sufficient label supervision in S while enabling the extraction of embeddings for training instances in Q. Results in Figure 4 (c)-(f) show that embeddings extracted by this strategy (with 10 folds) more faithfully capture dataset structure. We observe that TabPFN v2 simplifies the original tabular data distributions, transforming datasets into nearly linearly separable embedding spaces—especially after intermediate transformer layers.

We also experimented with a variant that uses the same context and query without partitioning, where the context contains all training samples and the query set includes both training and test points. This "non-partitioned" strategy improves upon the vanilla feature extraction baseline but still underperforms compared to our proposed leave-one-fold-out method. We attribute this to role ambiguity: query points that appear in the support set (either with dummy or ground-truth labels) are treated inconsistently, preventing the network from fully distinguishing between training and test roles and thereby degrading feature consistency. Detailed results for this variant are provided in the Appendix.

6.3 Validation of Embedding Quality

To validate the quality of the extracted embeddings, we train a logistic regression on embeddings derived from the training set and evaluate it on test set embeddings. The average rank across 29 classification datasets from the tiny benchmark2 in [75] is reported in Table 2.

Table 2: Average rank (lower is better) of TabPFN v2 and linear classifiers trained on the extracted embeddings across 29 classification datasets. Combined: embeddings from up to three layers (from the 12 available layers) are selected and concatenated, based on the validation set performance.

| ↓ Ta | bPFN v2 | 2 Vanilla | Layer 6 | Layer 9 | Layer 12 | Combined |
|------|---------|-----------|---------|---------|----------|----------|
| Rank | 2.69 | 5.97 | 4.28 | 4.00 | 2.12 | 1.94 |

Remarkably, training a simple linear classifier on the extracted embeddings achieves performance comparable to that of TabPFN v2's in-context learner. Furthermore, concatenating embeddings from multiple layers (e.g., both output and intermediate representations) can sometimes lead to even better results. These findings underscore TabPFN v2's potential as a strong and versatile feature encoder, suggesting broader applicability in downstream tasks such as tabular data analysis.

7 Improving TabPFN v2 via Test-Time Divide-and-Conquer

This section addresses the limitations discussed in Section 4.3, aiming to extend TabPFN v2's applicability beyond the boundaries. Specifically, we propose post-hoc divide-and-conquer strategies inspired by Chain-of-Thought (CoT) prompting [70], which decompose challenging tasks into simpler subtasks that TabPFN v2 can effectively handle.

7.1 High Dimension Datasets

High-dimensional datasets [36] present a unique challenge due to the quadratic complexity of TabPFN v2 with respect to the number of dimensions. To mitigate this, we propose subsampling the feature space into smaller subsets, processing each subset independently, and combining the predictions in an ensemble (bagging) fashion, similar to random forests [8].

In detail, we iteratively sample m subsets, each containing d' < d randomly selected attributes. For each subset, we leverage TabPFN v2's ability to handle lower-dimensional data to obtain predictions. We denote this divide-and-conquer and then ensemble strategy as TabPFN v2*, which aggregates outputs using averaging (for regression) or majority voting (for classification). To address high-dimensional tasks, we introduce a baseline variant, TabPFN v2-PCA, which incorporates dimensionality reduction. Specifically, TabPFN v2-PCA reduces the feature dimension to 500 using PCA to satisfy the input constraints of TabPFN v2. This process is repeated multiple times with different PCA projections, and the resulting predictions are aggregated via bagging to improve robustness.

Figure 5 (left) summarizes the results on 18 high-dimensional *classification* datasets. A variant that utilizes PCA to reduce the dimensionality, together with bagging, resolves the dimensionality issue to some extent. TabPFN v2* with d' = 500 and $m = \lceil d/d' \rceil$ significantly increases the mean accuracy (to the highest), effectively extending TabPFN v2's scalability to datasets with d > 2000.

7.2 Multi-Class Problems with More Than 10 Classes

To extend TabPFN v2 to tasks with more than 10 categories, we propose a decimal encoding approach that decomposes multi-class problems into multiple 10-class subproblems, ensuring compatibility with TabPFN v2's constraints.

For a task with C>10 classes, we encode each label $y\in [C]$ as a t-digit decimal representation, where $t=\lceil \log_{10} C \rceil$. For each digit position $j\in \{1,\ldots,t\}$, we train a separate TabPFN v2 model f_j to predict the j-th digit. During inference, the predicted digits are reconstructed to obtain the final class label. This strategy is also developed in [48], and we denote it as TabPFN v2-DPT. As the decimal encoding inherently introduces artificial correlations among classes — classes that share the same digit at a given position are grouped together, even if they are semantically unrelated. To mitigate this effect, our TabPFN v2* randomly permutes the class-to-digit mapping \sqrt{C} times, leading to different groupings in each run, and the prediction results are ensembles to improve robustness.

We consider the following variants of TabPFN v2 to address the 10-class limit in classification tasks:

- TabPFN v2-ECOC: We use the implementation provided in the official TabPFN extensions repository, which applies Error-Correcting Output Codes (ECOC).
- TabPFN v2-DPT: We encode each class label as a t-digit decimal string and train a separate TabPFN v2 to predict each digit. For instance, a 15-class problem is decomposed into two subproblems: one for the tens digit (classes $\{0,1\}$) and one for the ones digit (classes $\{0,\ldots,9\}$). The predicted digits are then decoded to recover the final class label.

We implement TabPFN v2 * based on TabPFN v2-DPT for efficiency. Specifically, TabPFN v2 * permutes the class-to-digit mapping \sqrt{C} times. For fair comparison, we also increase the number of ensembles in TabPFN v2-DPT to \sqrt{C} per digit to match the total number of predictions. As shown in Figure 5 (middle), this approach achieves the second-best mean accuracy on 12 datasets with more than 10 classes while preserving computational efficiency.

7.3 Large-Scale Datasets

For large-scale datasets, we randomly sample 10,000 training examples from the full training set as the support set and treat the remaining training examples and test instances as the query set. We extract their embeddings to form a new tabular dataset, on which a logistic regression classifier is trained to make predictions on the test set embeddings. This process is repeated four times, and the final predictions are aggregated. We denote this version as TabPFN v2*-SQ.

We also investigate integrating TabPFN v2 with decision trees to handle large-scale tasks. We note that a similar strategy was mentioned in [28] to handle within-dataset heterogeneity for a drastically different purpose. Specifically, we sample 32 subsets from the original training set, each containing

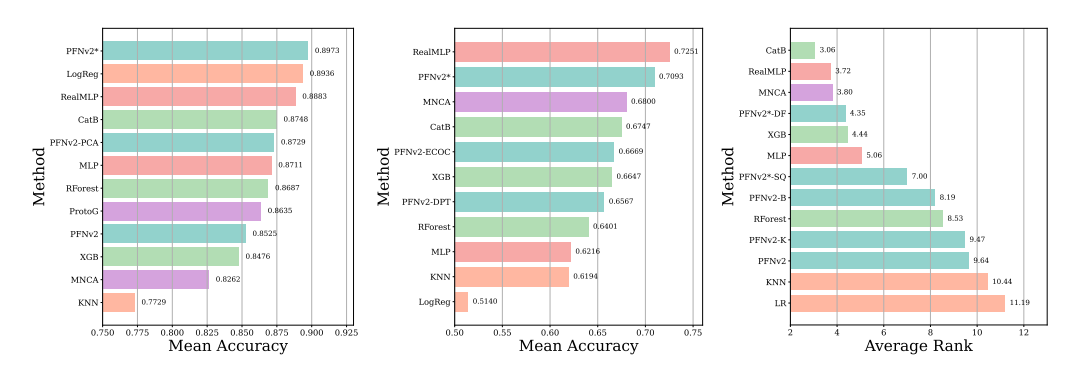


Figure 5: "*" indicates our extension. **Left**: Mean accuracy on 18 high-dimensional datasets. "-PCA" is another variant using PCA to reduce dimensions. **Middle**: Mean accuracy on 12 datasets with more than 10 classes. "-ECOC" denotes the multi-class ECOC strategy implemented by [28]. **Right**: Average rank on 18 large-scale datasets. "-B" refers to the variant that randomly subsamples 10,000 training examples four times and aggregates their predictions. "-K" denotes the variant that selects a representative subset of 10,000 training examples based on proximity to prototypes obtained via KMeans. All variants improve TabPFN v2.

60% of the original data (sampled without replacement). For each subset, we first train a shallow decision tree by setting the minimum number of samples required to split an internal node to 10,000. The decision tree partitions the training set into smaller, more manageable subsets. During inference, a test instance is first passed through each of the shallow decision tree to a leaf node and then predicted by the corresponding TabPFN v2 model. The predictions from all 32 models are aggregated. We denote this extension as TabPFN v2*-DF.

We consider the following variants of TabPFN v2 to scale to larger datasets:

- TabPFN v2-DT: A shallow decision tree is trained with a minimum split size of 10,000. The tree partitions the dataset into smaller subsets, and a separate TabPFN v2 model is applied to each leaf node. At inference, a test instance is routed through the tree to a corresponding leaf, where it is predicted by the respective TabPFN v2 model.
- TabPFN v2-B: A bagging-based variant that randomly samples 10,000 training examples four times and aggregates their predictions.
- TabPFN v2-K: Selects a representative subset of 10,000 training examples based on proximity to KMeans-derived prototypes.

Our TabPFN v2*-DF is an extension of TabPFN v2-DT to a forest-based ensemble. Specifically, we sample 32 subsets from the original training data, each containing 60% of the samples (without replacement), and train a separate TabPFN v2*-DT model on each subset. During inference, predictions from all 32 models are aggregated—*e.g.*, by majority voting or averaging—depending on the task type.

Figure 5 (right) shows the average rank results, including TabPFN v2*-SQ and TabPFN v2*-DF alongside variants using bagging and KMeans-based sampling. We observe that all variants improve upon the vanilla TabPFN v2 on large-scale datasets, with TabPFN v2*-DF and TabPFN v2*-SQ achieving the most significant improvement.

8 Conclusion

We present a timely investigation into TabPFN v2, a groundbreaking foundation model for tabular tasks. Our analysis uncovers the core mechanism behind TabPFN v2's strong performance across heterogeneous tabular datasets: it can infer attribute relationships on-the-fly—even from randomly initialized token inputs—without relying on pre-defined semantics or learning dataset-specific representations. We also demonstrate that TabPFN v2 can be repurposed as a powerful feature encoder, enabling broader applications such as data visualization and diagnostic analysis. To address its limitations in more complex data regimes, we introduce post-hoc divide-and-conquer strategies that extend TabPFN v2's utility without requiring model re-training. Together, these contributions offer fresh insights into advancing the development and application of foundation models for tabular data.

Acknowledgment

This work is partially supported by National Key R&D Program of China (2024YFE0202800), Collaborative Innovation Center of Novel Software Technology and Industrialization.

References

- [1] Takuya Akiba, Shotaro Sano, Toshihiko Yanase, Takeru Ohta, and Masanori Koyama. Optuna: A next-generation hyperparameter optimization framework. In *KDD*, pages 2623–2631, 2019.
- [2] Xavier Amatriain, Alejandro Jaimes, Nuria Oliver, and Josep M Pujol. Data mining methods for recommender systems. In *Recommender systems handbook*, pages 39–71. Springer, 2010.
- [3] Michael Arbel, David Salinas, and Frank Hutter. Equitabpfn: A target-permutation equivariant prior fitted networks. *CoRR*, abs/2502.06684, 2025.
- [4] Sercan Ö. Arik and Tomas Pfister. Tabnet: Attentive interpretable tabular learning. In *AAAI*, pages 6679–6687, 2021.
- [5] Sarkhan Badirli, Xuanqing Liu, Zhengming Xing, Avradeep Bhowmik, and Sathiya S. Keerthi. Gradient boosting neural networks: Grownet. *CoRR*, abs/2002.07971, 2020.
- [6] David Bonet, Daniel Mas Montserrat, Xavier Giró i Nieto, and Alexander G. Ioannidis. Hyperfast: Instant classification for tabular data. In *AAAI*, pages 11114–11123, 2024.
- [7] Vadim Borisov, Tobias Leemann, Kathrin Seßler, Johannes Haug, Martin Pawelczyk, and Gjergji Kasneci. Deep neural networks and tabular data: A survey. *IEEE Transactions Neural Networks and Learning Systems*, 35(6):7499–7519, 2024.
- [8] Leo Breiman. Random forests. *Machine Learning*, 45(1):5–32, 2001.
- [9] Jintai Chen, KuanLun Liao, Yanwen Fang, Danny Chen, and Jian Wu. Tabcaps: A capsule neural network for tabular data classification with bow routing. In *ICLR*, 2023.
- [10] Jintai Chen, Kuanlun Liao, Yao Wan, Danny Z. Chen, and Jian Wu. Danets: Deep abstract networks for tabular data classification and regression. In *AAAI*, pages 3930–3938, 2022.
- [11] Jintai Chen, Jiahuan Yan, Qiyuan Chen, Danny Ziyi Chen, Jian Wu, and Jimeng Sun. Can a deep learning model be a sure bet for tabular prediction? In *KDD*, pages 288–296, 2024.
- [12] Tianqi Chen and Carlos Guestrin. Xgboost: A scalable tree boosting system. In *KDD*, pages 785–794, 2016.
- [13] Manuel Fernández Delgado, Eva Cernadas, Senén Barro, and Dinani Gomes Amorim. Do we need hundreds of classifiers to solve real world classification problems? *Journal of Machine Learning Research*, 15(1):3133–3181, 2014.
- [14] Janez Demsar. Statistical comparisons of classifiers over multiple data sets. *Journal of Machine Learning Research*, 7:1–30, 2006.
- [15] Felix den Breejen, Sangmin Bae, Stephen Cha, and Se-Young Yun. Fine-tuned in-context learning transformers are excellent tabular data classifiers. *CoRR*, abs/2405.13396, 2025.
- [16] Benjamin Feuer, Chinmay Hegde, and Niv Cohen. Scaling tabpfn: Sketching and feature selection for tabular prior-data fitted networks. *CoRR*, abs/2311.10609, 2023.
- [17] Benjamin Feuer, Robin Tibor Schirrmeister, Valeriia Cherepanova, Chinmay Hegde, Frank Hutter, Micah Goldblum, Niv Cohen, and Colin White. Tunetables: Context optimization for scalable prior-data fitted networks. In *NeurIPS*, pages 83430–83464, 2024.
- [18] Matthias Feurer, Aaron Klein, Katharina Eggensperger, Jost Tobias Springenberg, Manuel Blum, and Frank Hutter. Efficient and robust automated machine learning. In *NIPS*, 2015.
- [19] Yury Gorishniy, Akim Kotelnikov, and Artem Babenko. Tabm: Advancing tabular deep learning with parameter-efficient ensembling. In *ICLR*, 2025.

- [20] Yury Gorishniy, Ivan Rubachev, and Artem Babenko. On embeddings for numerical features in tabular deep learning. In *NeurIPS*, pages 24991–25004, 2022.
- [21] Yury Gorishniy, Ivan Rubachev, Nikolay Kartashev, Daniil Shlenskii, Akim Kotelnikov, and Artem Babenko. Tabr: Tabular deep learning meets nearest neighbors in 2023. In *ICLR*, 2024.
- [22] Yury Gorishniy, Ivan Rubachev, Valentin Khrulkov, and Artem Babenko. Revisiting deep learning models for tabular data. In *NeurIPS*, pages 18932–18943, 2021.
- [23] Léo Grinsztajn, Edouard Oyallon, and Gaël Varoquaux. Why do tree-based models still outperform deep learning on typical tabular data? In *NeurIPS*, pages 507–520, 2022.
- [24] Isabelle Guyon, Lisheng Sun-Hosoya, Marc Boullé, Hugo Jair Escalante, Sergio Escalera, Zhengying Liu, Damir Jajetic, Bisakha Ray, Mehreen Saeed, Michèle Sebag, et al. Analysis of the automl challenge series. Automated Machine Learning, 177:177–219, 2019.
- [25] Sungwon Han, Jinsung Yoon, Sercan Ö. Arik, and Tomas Pfister. Large language models can automatically engineer features for few-shot tabular learning. In *ICML*, pages 17454–17479, 2024.
- [26] Stefan Hegselmann, Alejandro Buendia, Hunter Lang, Monica Agrawal, Xiaoyi Jiang, and David Sontag. Tabllm: few-shot classification of tabular data with large language models. In *AISTATS*, pages 5549–5581, 2023.
- [27] Noah Hollmann, Samuel Müller, Katharina Eggensperger, and Frank Hutter. Tabpfn: A transformer that solves small tabular classification problems in a second. In *ICLR*, 2023.
- [28] Noah Hollmann, Samuel Müller, Lennart Purucker, Arjun Krishnakumar, Max Körfer, Shi Bin Hoo, Robin Tibor Schirrmeister, and Frank Hutter. Accurate predictions on small data with a tabular foundation model. *Nature*, 637(8045):319–326, 2025.
- [29] David Holzmüller, Léo Grinsztajn, and Ingo Steinwart. Better by default: Strong pre-tuned mlps and boosted trees on tabular data. In *NeurIPS*, pages 26577–26658, 2024.
- [30] Shi Bin Hoo, Samuel Müller, David Salinas, and Frank Hutter. The tabular foundation model tabpfin outperforms specialized time series forecasting models based on simple features. *CoRR*, abs/2501.02945, 2025.
- [31] Xin Huang, Ashish Khetan, Milan Cvitkovic, and Zohar S. Karnin. Tabtransformer: Tabular data modeling using contextual embeddings. *CoRR*, abs/2012.06678, 2020.
- [32] Stephanie L Hyland, Martin Faltys, Matthias Hüser, Xinrui Lyu, Thomas Gumbsch, Cristóbal Esteban, Christian Bock, Max Horn, Michael Moor, Bastian Rieck, et al. Early prediction of circulatory failure in the intensive care unit using machine learning. *Nature medicine*, 26(3):364–373, 2020.
- [33] Ovidiu Ivanciuc et al. Applications of support vector machines in chemistry. *Reviews in computational chemistry*, 23:291, 2007.
- [34] Tomoharu Iwata and Atsutoshi Kumagai. Meta-learning from tasks with heterogeneous attribute spaces. In *NeurIPS*, pages 6053–6063, 2020.
- [35] Alan Jeffares, Tennison Liu, Jonathan Crabbé, Fergus Imrie, and Mihaela van der Schaar. Tangos: Regularizing tabular neural networks through gradient orthogonalization and specialization. In *ICLR*, 2023.
- [36] Xiangjian Jiang, Andrei Margeloiu, Nikola Simidjievski, and Mateja Jamnik. Protogate: Prototype-based neural networks with global-to-local feature selection for tabular biomedical data. In *ICML*, pages 21844–21878, 2024.
- [37] Arlind Kadra, Marius Lindauer, Frank Hutter, and Josif Grabocka. Well-tuned simple nets excel on tabular datasets. In *NeurIPS*, pages 23928–23941, 2021.

- [38] Guolin Ke, Qi Meng, Thomas Finley, Taifeng Wang, Wei Chen, Weidong Ma, Qiwei Ye, and Tie-Yan Liu. Lightgbm: A highly efficient gradient boosting decision tree. In NIPS, pages 3146–3154, 2017.
- [39] Myung Jun Kim, Léo Grinsztajn, and Gaël Varoquaux. CARTE: pretraining and transfer for tabular learning. In ICML, pages 23843–23866, 2024.
- [40] Alexander Kirillov, Eric Mintun, Nikhila Ravi, Hanzi Mao, Chloé Rolland, Laura Gustafson, Tete Xiao, Spencer Whitehead, Alexander C. Berg, Wan-Yen Lo, Piotr Dollár, and Ross B. Girshick. Segment anything. In *ICCV*, pages 3992–4003, 2023.
- [41] Günter Klambauer, Thomas Unterthiner, Andreas Mayr, and Sepp Hochreiter. Self-normalizing neural networks. In *NIPS*, pages 971–980, 2017.
- [42] Ravin Kohli, Matthias Feurer, Katharina Eggensperger, Bernd Bischl, and Frank Hutter. Towards quantifying the effect of datasets for benchmarking: A look at tabular machine learning. In *ICLR Workshop*, 2024.
- [43] Boris Kovalerchuk and Evgenii Vityaev. *Data mining in finance: advances in relational and hybrid methods*. Springer Science & Business Media, 2005.
- [44] Lang Liu, Mahdi Milani Fard, and Sen Zhao. Distribution embedding networks for generalization from a diverse set of classification tasks. *Transactions on Machine Learning Research*, 2022.
- [45] Si-Yang Liu and Han-Jia Ye. Tabpfn unleashed: A scalable and effective solution to tabular classification problems. *CoRR*, abs/2502.02527, 2025.
- [46] Si-Yang Liu and Han-Jia Ye. Tabpfn unleashed: A scalable and effective solution to tabular classification problems. In *ICML*, 2025.
- [47] Junwei Ma, Apoorv Dankar, George Stein, Guangwei Yu, and Anthony L. Caterini. Tabpfgen tabular data generation with tabpfn. *CoRR*, abs/2406.05216, 2024.
- [48] Junwei Ma, Valentin Thomas, Rasa Hosseinzadeh, Hamidreza Kamkari, Alex Labach, Jesse C. Cresswell, Keyvan Golestan, Guangwei Yu, Maksims Volkovs, and Anthony L. Caterini. Tabdpt: Scaling tabular foundation models. *CoRR*, abs/2410.18164, 2024.
- [49] Duncan C. McElfresh, Sujay Khandagale, Jonathan Valverde, Vishak Prasad C., Ganesh Ramakrishnan, Micah Goldblum, and Colin White. When do neural nets outperform boosted trees on tabular data? In *NeurIPS*, pages 76336–76369, 2023.
- [50] Andreas C. Mueller, Carlo Curino, and Raghu Ramakrishnan. Mothernet: Fast training and inference via hyper-network transformers. In *ICLR*, 2025.
- [51] Niklas Muennighoff, Zitong Yang, Weijia Shi, Xiang Lisa Li, Li Fei-Fei, Hannaneh Hajishirzi, Luke Zettlemoyer, Percy Liang, Emmanuel Candès, and Tatsunori Hashimoto. s1: Simple test-time scaling. *CoRR*, abs/2501.19393, 2025.
- [52] Youssef Nader, Leon Sixt, and Tim Landgraf. DNNR: differential nearest neighbors regression. In *ICML*, pages 16296–16317, 2022.
- [53] Thomas Nagler. Statistical foundations of prior-data fitted networks. In Andreas Krause, Emma Brunskill, Kyunghyun Cho, Barbara Engelhardt, Sivan Sabato, and Jonathan Scarlett, editors, ICML, pages 25660–25676, 2023.
- [54] Soma Onishi, Kenta Oono, and Kohei Hayashi. Tabret: Pre-training transformer-based tabular models for unseen columns. *CoRR*, abs/2303.15747, 2023.
- [55] Sergei Popov, Stanislav Morozov, and Artem Babenko. Neural oblivious decision ensembles for deep learning on tabular data. In *ICLR*, 2020.
- [56] Liudmila Ostroumova Prokhorenkova, Gleb Gusev, Aleksandr Vorobev, Anna Veronika Dorogush, and Andrey Gulin. Catboost: unbiased boosting with categorical features. In *NeurIPS*, pages 6639–6649, 2018.

- [57] Jingang Qu, David Holzmüller, Gaël Varoquaux, and Marine Le Morvan. Tabicl: A tabular foundation model for in-context learning on large data. In *ICML*, 2025.
- [58] Cristóbal Romero and Sebastián Ventura. Educational data mining: a review of the state of the art. IEEE Transactions on Systems, Man, and Cybernetics, 40(6):601–618, 2010.
- [59] Ivan Rubachev, Artem Alekberov, Yury Gorishniy, and Artem Babenko. Revisiting pretraining objectives for tabular deep learning. *CoRR*, abs/2207.03208, 2022.
- [60] Ivan Rubachev, Nikolay Kartashev, Yury Gorishniy, and Artem Babenko. Tabred: A benchmark of tabular machine learning in-the-wild. In ICLR, 2025.
- [61] Sergio Ruiz-Villafranca, José Roldán Gómez, Juan Manuel Castelo Gómez, Javier Carrillo Mondéjar, and José Luis Martínez. A tabpfn-based intrusion detection system for the industrial internet of things. *The Journal of Supercomputing*, 80(14):20080–20117, 2024.
- [62] Junhong Shen, Liam Li, Lucio M Dery, Corey Staten, Mikhail Khodak, Graham Neubig, and Ameet Talwalkar. Cross-modal fine-tuning: Align then refine. In *ICML*, pages 31030–31056, 2023.
- [63] Gowthami Somepalli, Avi Schwarzschild, Micah Goldblum, C. Bayan Bruss, and Tom Goldstein. SAINT: Improved neural networks for tabular data via row attention and contrastive pre-training. In *NeurIPS Workshop*, 2022.
- [64] Weiping Song, Chence Shi, Zhiping Xiao, Zhijian Duan, Yewen Xu, Ming Zhang, and Jian Tang. Autoint: Automatic feature interaction learning via self-attentive neural networks. In *CIKM*, pages 1161–1170, 2019.
- [65] Valentin Thomas, Junwei Ma, Rasa Hosseinzadeh, Keyvan Golestan, Guangwei Yu, Maksims Volkovs, and Anthony L. Caterini. Retrieval & fine-tuning for in-context tabular models. In *NeurIPS*, pages 108439–108467, 2024.
- [66] Boris van Breugel and Mihaela van der Schaar. Position: Why tabular foundation models should be a research priority. In *ICML*, pages 48976–48993, 2024.
- [67] Ashish Vaswani, Noam Shazeer, Niki Parmar, Jakob Uszkoreit, Llion Jones, Aidan N Gomez, Łukasz Kaiser, and Illia Polosukhin. Attention is all you need. In NIPS, 2017.
- [68] Ruoxi Wang, Rakesh Shivanna, Derek Zhiyuan Cheng, Sagar Jain, Dong Lin, Lichan Hong, and Ed H. Chi. DCN V2: improved deep & cross network and practical lessons for web-scale learning to rank systems. In WWW, pages 1785–1797, 2021.
- [69] Zifeng Wang, Chufan Gao, Cao Xiao, and Jimeng Sun. Anypredict: Foundation model for tabular prediction. *CoRR*, abs/2305.12081, 2023.
- [70] Jason Wei, Xuezhi Wang, Dale Schuurmans, Maarten Bosma, Brian Ichter, Fei Xia, Ed H. Chi, Quoc V. Le, and Denny Zhou. Chain-of-thought prompting elicits reasoning in large language models. In *NeurIPS*, pages 24824–24837, 2022.
- [71] Xumeng Wen, Han Zhang, Shun Zheng, Wei Xu, and Jiang Bian. From supervised to generative: A novel paradigm for tabular deep learning with large language models. In *KDD*, pages 3323–3333, 2024.
- [72] Jing Wu, Suiyao Chen, Qi Zhao, Renat Sergazinov, Chen Li, Shengjie Liu, Chongchao Zhao, Tianpei Xie, Hanqing Guo, Cheng Ji, Daniel Cociorva, and Hakan Brunzell. Switchtab: Switched autoencoders are effective tabular learners. In *AAAI*, pages 15924–15933, 2024.
- [73] Derek Xu, Olcay Cirit, Reza Asadi, Yizhou Sun, and Wei Wang. Mixture of in-context prompters for tabular pfns. *CoRR*, abs/2405.16156, 2024.
- [74] Jiahuan Yan, Bo Zheng, Hongxia Xu, Yiheng Zhu, Danny Z. Chen, Jimeng Sun, Jian Wu, and Jintai Chen. Making pre-trained language models great on tabular prediction. In *ICLR*, 2024.
- [75] Han-Jia Ye, Si-Yang Liu, Hao-Run Cai, Qi-Le Zhou, and De-Chuan Zhan. A closer look at deep learning on tabular data. *CoRR*, abs/2407.00956, 2024.

- [76] Han-Jia Ye, Huai-Hong Yin, De-Chuan Zhan, and Wei-Lun Chao. Revisiting nearest neighbor for tabular data: A deep tabular baseline two decades later. In *ICLR*, 2025.
- [77] Han-Jia Ye, Qi-Le Zhou, Huai-Hong Yin, De-Chuan Zhan, and Wei-Lun Chao. Rethinking pre-training in tabular data: A neighborhood embedding perspective. *CoRR*, abs/2311.00055, 2025.
- [78] Hangting Ye, Wei Fan, Xiaozhuang Song, Shun Zheng, He Zhao, Dan dan Guo, and Yi Chang. Ptarl: Prototype-based tabular representation learning via space calibration. In *ICLR*, 2024.
- [79] Tianping Zhang, Shaowen Wang, Shuicheng Yan, Jian Li, and Qian Liu. Generative table pre-training empowers models for tabular prediction. In *EMNLP*, pages 14836–14854, 2023.
- [80] Yiyuan Zhang, Kaixiong Gong, Kaipeng Zhang, Hongsheng Li, Yu Qiao, Wanli Ouyang, and Xiangyu Yue. Meta-transformer: A unified framework for multimodal learning. CoRR, abs/2307.10802, 2023.
- [81] Ce Zhou, Qian Li, Chen Li, Jun Yu, Yixin Liu, Guangjing Wang, Kai Zhang, Cheng Ji, Qiben Yan, Lifang He, et al. A comprehensive survey on pretrained foundation models: A history from bert to chatgpt. *International Journal of Machine Learning and Cybernetics*, pages 1–65, 2024.
- [82] Bingzhao Zhu, Xingjian Shi, Nick Erickson, Mu Li, George Karypis, and Mahsa Shoaran. Xtab: Cross-table pretraining for tabular transformers. In *ICML*, pages 43181–43204, 2023.

NeurIPS Paper Checklist

1. Claims

Question: Do the main claims made in the abstract and introduction accurately reflect the paper's contributions and scope?

Answer: [Yes]

Justification: The abstract and introduction state the claims made, including the contributions made in the paper and important assumptions and limitations.

Guidelines:

- The answer NA means that the abstract and introduction do not include the claims made in the paper.
- The abstract and/or introduction should clearly state the claims made, including the contributions made in the paper and important assumptions and limitations. A No or NA answer to this question will not be perceived well by the reviewers.
- The claims made should match theoretical and experimental results, and reflect how much the results can be expected to generalize to other settings.
- It is fine to include aspirational goals as motivation as long as it is clear that these goals
 are not attained by the paper.

2. Limitations

Question: Does the paper discuss the limitations of the work performed by the authors?

Answer: [Yes]

Justification: In Appendix.

- The answer NA means that the paper has no limitation while the answer No means that the paper has limitations, but those are not discussed in the paper.
- The authors are encouraged to create a separate "Limitations" section in their paper.
- The paper should point out any strong assumptions and how robust the results are to violations of these assumptions (e.g., independence assumptions, noiseless settings, model well-specification, asymptotic approximations only holding locally). The authors should reflect on how these assumptions might be violated in practice and what the implications would be.

- The authors should reflect on the scope of the claims made, e.g., if the approach was
 only tested on a few datasets or with a few runs. In general, empirical results often
 depend on implicit assumptions, which should be articulated.
- The authors should reflect on the factors that influence the performance of the approach. For example, a facial recognition algorithm may perform poorly when image resolution is low or images are taken in low lighting. Or a speech-to-text system might not be used reliably to provide closed captions for online lectures because it fails to handle technical jargon.
- The authors should discuss the computational efficiency of the proposed algorithms and how they scale with dataset size.
- If applicable, the authors should discuss possible limitations of their approach to address problems of privacy and fairness.
- While the authors might fear that complete honesty about limitations might be used by reviewers as grounds for rejection, a worse outcome might be that reviewers discover limitations that aren't acknowledged in the paper. The authors should use their best judgment and recognize that individual actions in favor of transparency play an important role in developing norms that preserve the integrity of the community. Reviewers will be specifically instructed to not penalize honesty concerning limitations.

3. Theory assumptions and proofs

Question: For each theoretical result, does the paper provide the full set of assumptions and a complete (and correct) proof?

Answer: [NA]

Justification: This paper does not include theoretical results.

Guidelines:

- The answer NA means that the paper does not include theoretical results.
- All the theorems, formulas, and proofs in the paper should be numbered and crossreferenced.
- All assumptions should be clearly stated or referenced in the statement of any theorems.
- The proofs can either appear in the main paper or the supplemental material, but if they appear in the supplemental material, the authors are encouraged to provide a short proof sketch to provide intuition.
- Inversely, any informal proof provided in the core of the paper should be complemented by formal proofs provided in appendix or supplemental material.
- Theorems and Lemmas that the proof relies upon should be properly referenced.

4. Experimental result reproducibility

Question: Does the paper fully disclose all the information needed to reproduce the main experimental results of the paper to the extent that it affects the main claims and/or conclusions of the paper (regardless of whether the code and data are provided or not)?

Answer: [Yes]

Justification: We have disclosed all key information necessary to reproduce the experimental results.

- The answer NA means that the paper does not include experiments.
- If the paper includes experiments, a No answer to this question will not be perceived well by the reviewers: Making the paper reproducible is important, regardless of whether the code and data are provided or not.
- If the contribution is a dataset and/or model, the authors should describe the steps taken to make their results reproducible or verifiable.
- Depending on the contribution, reproducibility can be accomplished in various ways.
 For example, if the contribution is a novel architecture, describing the architecture fully might suffice, or if the contribution is a specific model and empirical evaluation, it may be necessary to either make it possible for others to replicate the model with the same dataset, or provide access to the model. In general, releasing code and data is often

one good way to accomplish this, but reproducibility can also be provided via detailed instructions for how to replicate the results, access to a hosted model (e.g., in the case of a large language model), releasing of a model checkpoint, or other means that are appropriate to the research performed.

- While NeurIPS does not require releasing code, the conference does require all submissions to provide some reasonable avenue for reproducibility, which may depend on the nature of the contribution. For example
 - (a) If the contribution is primarily a new algorithm, the paper should make it clear how to reproduce that algorithm.
- (b) If the contribution is primarily a new model architecture, the paper should describe the architecture clearly and fully.
- (c) If the contribution is a new model (e.g., a large language model), then there should either be a way to access this model for reproducing the results or a way to reproduce the model (e.g., with an open-source dataset or instructions for how to construct the dataset).
- (d) We recognize that reproducibility may be tricky in some cases, in which case authors are welcome to describe the particular way they provide for reproducibility. In the case of closed-source models, it may be that access to the model is limited in some way (e.g., to registered users), but it should be possible for other researchers to have some path to reproducing or verifying the results.

5. Open access to data and code

Question: Does the paper provide open access to the data and code, with sufficient instructions to faithfully reproduce the main experimental results, as described in supplemental material?

Answer: [NA]

Justification: We provide sufficient instructions to faithfully reproduce the main experimental results.

Guidelines:

- The answer NA means that paper does not include experiments requiring code.
- Please see the NeurIPS code and data submission guidelines (https://nips.cc/public/guides/CodeSubmissionPolicy) for more details.
- While we encourage the release of code and data, we understand that this might not be possible, so "No" is an acceptable answer. Papers cannot be rejected simply for not including code, unless this is central to the contribution (e.g., for a new open-source benchmark).
- The instructions should contain the exact command and environment needed to run to reproduce the results. See the NeurIPS code and data submission guidelines (https://nips.cc/public/guides/CodeSubmissionPolicy) for more details.
- The authors should provide instructions on data access and preparation, including how to access the raw data, preprocessed data, intermediate data, and generated data, etc.
- The authors should provide scripts to reproduce all experimental results for the new proposed method and baselines. If only a subset of experiments are reproducible, they should state which ones are omitted from the script and why.
- At submission time, to preserve anonymity, the authors should release anonymized versions (if applicable).
- Providing as much information as possible in supplemental material (appended to the paper) is recommended, but including URLs to data and code is permitted.

6. Experimental setting/details

Question: Does the paper specify all the training and test details (e.g., data splits, hyperparameters, how they were chosen, type of optimizer, etc.) necessary to understand the results?

Answer: [Yes]

Justification: In Appendix.

- The answer NA means that the paper does not include experiments.
- The experimental setting should be presented in the core of the paper to a level of detail that is necessary to appreciate the results and make sense of them.
- The full details can be provided either with the code, in appendix, or as supplemental
 material.

7. Experiment statistical significance

Question: Does the paper report error bars suitably and correctly defined or other appropriate information about the statistical significance of the experiments?

Answer: [Yes]

Justification: In Appendix.

Guidelines:

- The answer NA means that the paper does not include experiments.
- The authors should answer "Yes" if the results are accompanied by error bars, confidence intervals, or statistical significance tests, at least for the experiments that support the main claims of the paper.
- The factors of variability that the error bars are capturing should be clearly stated (for example, train/test split, initialization, random drawing of some parameter, or overall run with given experimental conditions).
- The method for calculating the error bars should be explained (closed form formula, call to a library function, bootstrap, etc.)
- The assumptions made should be given (e.g., Normally distributed errors).
- It should be clear whether the error bar is the standard deviation or the standard error
 of the mean.
- It is OK to report 1-sigma error bars, but one should state it. The authors should preferably report a 2-sigma error bar than state that they have a 96% CI, if the hypothesis of Normality of errors is not verified.
- For asymmetric distributions, the authors should be careful not to show in tables or figures symmetric error bars that would yield results that are out of range (e.g. negative error rates).
- If error bars are reported in tables or plots, The authors should explain in the text how they were calculated and reference the corresponding figures or tables in the text.

8. Experiments compute resources

Question: For each experiment, does the paper provide sufficient information on the computer resources (type of compute workers, memory, time of execution) needed to reproduce the experiments?

Answer: [Yes]

Justification: In Appendix.

Guidelines:

- The answer NA means that the paper does not include experiments.
- The paper should indicate the type of compute workers CPU or GPU, internal cluster, or cloud provider, including relevant memory and storage.
- The paper should provide the amount of compute required for each of the individual experimental runs as well as estimate the total compute.
- The paper should disclose whether the full research project required more compute than the experiments reported in the paper (e.g., preliminary or failed experiments that didn't make it into the paper).

9. Code of ethics

Question: Does the research conducted in the paper conform, in every respect, with the NeurIPS Code of Ethics https://neurips.cc/public/EthicsGuidelines?

Answer: [Yes]

Justification: We make sure that we preserve anonymity.

Guidelines:

- The answer NA means that the authors have not reviewed the NeurIPS Code of Ethics.
- If the authors answer No, they should explain the special circumstances that require a
 deviation from the Code of Ethics.
- The authors should make sure to preserve anonymity (e.g., if there is a special consideration due to laws or regulations in their jurisdiction).

10. Broader impacts

Question: Does the paper discuss both potential positive societal impacts and negative societal impacts of the work performed?

Answer: [Yes]

Justification: In Appendix.

Guidelines:

- The answer NA means that there is no societal impact of the work performed.
- If the authors answer NA or No, they should explain why their work has no societal impact or why the paper does not address societal impact.
- Examples of negative societal impacts include potential malicious or unintended uses (e.g., disinformation, generating fake profiles, surveillance), fairness considerations (e.g., deployment of technologies that could make decisions that unfairly impact specific groups), privacy considerations, and security considerations.
- The conference expects that many papers will be foundational research and not tied to particular applications, let alone deployments. However, if there is a direct path to any negative applications, the authors should point it out. For example, it is legitimate to point out that an improvement in the quality of generative models could be used to generate deepfakes for disinformation. On the other hand, it is not needed to point out that a generic algorithm for optimizing neural networks could enable people to train models that generate Deepfakes faster.
- The authors should consider possible harms that could arise when the technology is being used as intended and functioning correctly, harms that could arise when the technology is being used as intended but gives incorrect results, and harms following from (intentional or unintentional) misuse of the technology.
- If there are negative societal impacts, the authors could also discuss possible mitigation strategies (e.g., gated release of models, providing defenses in addition to attacks, mechanisms for monitoring misuse, mechanisms to monitor how a system learns from feedback over time, improving the efficiency and accessibility of ML).

11. Safeguards

Question: Does the paper describe safeguards that have been put in place for responsible release of data or models that have a high risk for misuse (e.g., pretrained language models, image generators, or scraped datasets)?

Answer: [NA]

Justification: The paper poses no such risks.

Guidelines:

- The answer NA means that the paper poses no such risks.
- Released models that have a high risk for misuse or dual-use should be released with
 necessary safeguards to allow for controlled use of the model, for example by requiring
 that users adhere to usage guidelines or restrictions to access the model or implementing
 safety filters.
- Datasets that have been scraped from the Internet could pose safety risks. The authors should describe how they avoided releasing unsafe images.
- We recognize that providing effective safeguards is challenging, and many papers do
 not require this, but we encourage authors to take this into account and make a best
 faith effort.

12. Licenses for existing assets

Question: Are the creators or original owners of assets (e.g., code, data, models), used in the paper, properly credited and are the license and terms of use explicitly mentioned and properly respected?

Answer: [Yes]

Justification: We are confident that the creators or original owners of assets (e.g., code, data, models) used in the paper are properly credited, and the license and terms of use are explicitly mentioned and properly respected.

Guidelines:

- The answer NA means that the paper does not use existing assets.
- The authors should cite the original paper that produced the code package or dataset.
- The authors should state which version of the asset is used and, if possible, include a URL.
- The name of the license (e.g., CC-BY 4.0) should be included for each asset.
- For scraped data from a particular source (e.g., website), the copyright and terms of service of that source should be provided.
- If assets are released, the license, copyright information, and terms of use in the
 package should be provided. For popular datasets, paperswithcode.com/datasets
 has curated licenses for some datasets. Their licensing guide can help determine the
 license of a dataset.
- For existing datasets that are re-packaged, both the original license and the license of the derived asset (if it has changed) should be provided.
- If this information is not available online, the authors are encouraged to reach out to the asset's creators.

13. New assets

Question: Are new assets introduced in the paper well documented and is the documentation provided alongside the assets?

Answer: [NA]

Justification: The paper does not release new assets.

Guidelines:

- The answer NA means that the paper does not release new assets.
- Researchers should communicate the details of the dataset/code/model as part of their submissions via structured templates. This includes details about training, license, limitations, etc.
- The paper should discuss whether and how consent was obtained from people whose asset is used.
- At submission time, remember to anonymize your assets (if applicable). You can either create an anonymized URL or include an anonymized zip file.

14. Crowdsourcing and research with human subjects

Question: For crowdsourcing experiments and research with human subjects, does the paper include the full text of instructions given to participants and screenshots, if applicable, as well as details about compensation (if any)?

Answer: [NA]

Justification: This paper does not use crowdsourcing nor research with human subjects.

- The answer NA means that the paper does not involve crowdsourcing nor research with human subjects.
- Including this information in the supplemental material is fine, but if the main contribution of the paper involves human subjects, then as much detail as possible should be included in the main paper.
- According to the NeurIPS Code of Ethics, workers involved in data collection, curation, or other labor should be paid at least the minimum wage in the country of the data collector.

15. Institutional review board (IRB) approvals or equivalent for research with human subjects

Question: Does the paper describe potential risks incurred by study participants, whether such risks were disclosed to the subjects, and whether Institutional Review Board (IRB) approvals (or an equivalent approval/review based on the requirements of your country or institution) were obtained?

Answer: [NA]

Justification: This paper does not involve crowdsourcing nor research with human subjects. Guidelines:

- The answer NA means that the paper does not involve crowdsourcing nor research with human subjects.
- Depending on the country in which research is conducted, IRB approval (or equivalent) may be required for any human subjects research. If you obtained IRB approval, you should clearly state this in the paper.
- We recognize that the procedures for this may vary significantly between institutions and locations, and we expect authors to adhere to the NeurIPS Code of Ethics and the guidelines for their institution.
- For initial submissions, do not include any information that would break anonymity (if applicable), such as the institution conducting the review.

16. Declaration of LLM usage

Question: Does the paper describe the usage of LLMs if it is an important, original, or non-standard component of the core methods in this research? Note that if the LLM is used only for writing, editing, or formatting purposes and does not impact the core methodology, scientific rigorousness, or originality of the research, declaration is not required.

Answer: [NA]

Justification: In this work, the LLM is used only for writing, editing, or formatting purposes and does not impact the core methodology, scientific rigorousness, or originality of the research.

- The answer NA means that the core method development in this research does not involve LLMs as any important, original, or non-standard components.
- Please refer to our LLM policy (https://neurips.cc/Conferences/2025/LLM) for what should or should not be described.

In the appendix, we provide additional details, discussions, and experimental results to complement the main paper:

- Appendix A: Additional related work and discussions on methods closely related to our study (cf. Section 2 of the main paper).
- Appendix B: Detailed descriptions of the comparison methods used in our evaluation (cf. Section 4 of the main paper).
- Appendix C: Additional qualitative and quantitative results for feature extraction using TabPFN v2, supplementing Section 6 of the main paper.
- Appendix D: Analysis of the impact of feature engineering and ensemble strategies in TabPFN v2, as well as a meta-feature-based analysis to identify the conditions under which TabPFN v2 performs well or poorly.
- Appendix E: Complete results corresponding to the tables and figures referenced in the main paper.
- Appendix F: Limitation and social impact of the paper.

A Additional Related Work

Learning with Tabular Data. Tabular data is prevalent across diverse fields, including healthcare, finance, and education [43, 32, 58, 2]. Tree-based models, such as XGBoost [12], LightGBM [38], and CatBoost [56], have long dominated this domain. However, recent advances in deep neural networks (DNNs) have demonstrated strong potential for tabular data [7]. Popular architectures like multi-layer perceptrons [22, 37] and Transformers [31] have been adapted to tabular tasks, alongside custom architectures designed specifically for tabular data [41, 68].

Deep tabular methods can be broadly categorized into two types. The first type directly processes raw features [29, 21, 76], sometimes incorporating feature-specific encoding strategies [20]. The second type tokenizes features, transforming an example into a set of tokens [64, 31, 59]. Comprehensive benchmarks have been developed to evaluate these methods across diverse datasets [23, 49, 75, 60], highlighting the strengths and weaknesses of deep tabular models in various scenarios.

Variants of TabPFN. TabPFN's success stems from its pre-training on massive synthetic datasets, enabling strong in-context learning performance on small-scale classification tasks [27]. Motivated by its capabilities, researchers have explored a variety of applications, including tabular data generation [47], anomaly detection [61], and time series forecasting [30]. [53] provided a bias-variance analysis of TabPFN, offering insight into its generalization behavior. Another line of research focuses on improving scalability by addressing TabPFN's sensitivity to context size [16, 73]. Further strategies to enhance downstream performance include context adaptation with nearest neighbor [65], partial fine-tuning [17, 45], pre-training on real-world datasets [48], scalable ensemble [46], and more powerful and efficient pre-training on synthetic data [57]. Most of these variants remain restricted to classification tasks due to limitations in TabPFN v1.

The recently introduced TabPFN v2 [28] extends TabPFN to support regression tasks and accommodate larger context sizes. In this paper, we conduct a comprehensive evaluation of TabPFN v2, analyze its strengths, and introduce methods to overcome its scalability and applicability challenges.

B Evaluation Details

Experimental Compute Resources. All experiments were conducted using 4 NVIDIA RTX 6000 Ada GPUs and 2 Intel(R) Xeon(R) Platinum 8352V CPUs.

Please refer [75] for details of the 300 small to medium datasets. For high-dimensional datasets, we selected 18 datasets with more than 2000 features from the scikit-feature repository. Detailed statistics of high-dimensional datasets and large-scale datasets are reported in Table 3 and Table 4.

We follow [75] and use different colors to represent various categories of methods in the result figures, ensuring clarity and easy comparison. In Figure 1 (right) and Figure 2 of the main paper, we compare the following methods:

Table 3: Dataset Information for High-Dimensional Data Experiments: A collection of 18 datasets with varying numbers of instances, features, and classes used in our high-dimensional experiments.

| Dataset | #Instances | #Features | #Classes Dataset | | #Instances | #Features | #Classes |
|-------------|------------|-----------|--------------------|-------------|------------|-----------|----------|
| BASEHOCK | 1993 | 4862 | 2 | lung | 203 | 3312 | 5 |
| PCMAC | 1943 | 3289 | 2 | warpPIE10P | 210 | 2420 | 10 |
| RELATHE | 1427 | 4322 | 2 | orlraws10P | 100 | 10304 | 10 |
| ALLAML | 72 | 7129 | 2 | Prostate_GE | 102 | 5966 | 2 |
| CLL_SUB_111 | 111 | 11340 | 3 | SMK_CAN_187 | 187 | 19993 | 2 |
| colon | 62 | 2000 | 2 | warpAR10P | 130 | 2400 | 10 |
| GLI_85 | 85 | 22283 | 2 | arcene | 200 | 10000 | 2 |
| GLIOMA | 50 | 4434 | 4 | gisette | 7000 | 5000 | 2 |
| leukemia | 72 | 7070 | 2 | TOX_171 | 171 | 5748 | 4 |

Table 4: Dataset Information for Large-scale Data Experiments.

| | | | | • | | | |
|-------------------|------------|-----------|----------|---------------------|------------|-----------|----------|
| Dataset | #Instances | #Features | #Classes | Dataset | #Instances | #Features | #Classes |
| BNG(credit-a) | 1,000,000 | 15 | 2 | CDC_Indicators | 253,680 | 21 | 2 |
| Higgs | 1,000,000 | 28 | 2 | Smoking_signal | 991,346 | 23 | 2 |
| nomao | 34,465 | 118 | 2 | sf-police-incidents | 2,215,023 | 8 | 2 |
| Data_Crowdfunding | 671,025 | 11 | 4 | Fashion-MNIST | 70,000 | 784 | 10 |
| covertype | 581,012 | 54 | 7 | jannis | 83,733 | 54 | 4 |
| poker-hand | 1,025,009 | 10 | 10 | volkert | 58,310 | 180 | 10 |
| Airlines_DepDelay | 10,000,000 | 9 | - | Wave_Energy_Farm | 36,043 | 99 | - |
| UJIndoorLoc | 21,048 | 520 | - | blogfeedback | 60,021 | 276 | - |
| microsoft | 1,200,192 | 136 | - | yahoo | 709,877 | 699 | - |
| | | | | | | | |

- Classical Methods (): The classical methods include Dummy, Logistic Regression (LR), K-Nearest Neighbors (KNN), Support Vector Machines (SVM), Naive Bayes, Linear Regression, and DNNR [52], which serve as basic baselines for classification and regression tasks.
- Tree-based Methods (): Tree-based methods such as Random Forest [8], XGBoost [12], Light-GBM [38], and CatBoost [56] are known for their high performance on tabular data.
- MLP variants (): MLP variants, including vanilla MLP, MLP-PLR, Self-Normalizing Neural Networks [41], Residual Network [22], and TabM [19] enhance the flexibility and generalization of traditional MLP architectures through advanced regularization and residual connections.
- Special Architectures (): Methods with specially designed architectures, such as DCNv2 [68], DANets [10], and TabCaps [9], focus on improving feature interaction and abstraction to capture complex relationships in tabular data.
- Token-based Methods (): Token-based methods like AutoInt [64], TabTransformer [31], FT-Transformer [22], and ExcelFormer [11] represent features as tokens, enabling models to capture higher-order interactions through attention mechanisms.
- Regularization-based Methods (): Regularization-based methods, including TANGOS [35], SwitchTab [72], and PTaRL [78], aim to improve model generalization by incorporating regularization techniques during training to enhance the robustness of predictions.
- Tree-mimic Methods (): Tree-mimic methods, such as NODE [55], GrowNet [5], and TabNet [4], combine the interpretability of decision trees with the power of deep learning, employing attention mechanisms to select important features.
- Context-based Methods (): Context-based methods like TabR [21] and ModernNCA [76] leverage contextual information from the training data to improve predictions by utilizing neighborhood-based and in-context learning strategies.

In addition to the aforementioned methods, for other experimental results, we will demonstrate the performance of **TabPFN v2 and its variants**, which are represented by emerald teal (), ensuring that their experimental effects are clearly distinguished from the other methods.

Remark. The standard checkpoint released by TabPFN employs a feature grouping size of 2, which complicates the analysis of individual feature embeddings and inter-feature relationships. To facilitate such analysis, we use a modified checkpoint with *group size=1* for the experiments in Figure 3 of the main paper, which is available at HuggingFace.

C Additional Feature Extraction Results

In this section, we provide further results on regression tasks and additional variants of our feature extraction strategy to validate the effectiveness and robustness of the proposed leave-one-fold-out method with TabPFN v2. We also compare this supervised approach to two unsupervised embedding extraction methods, as well as a non-partitioned variant that uses the same context and query without data folding.

C.1 Additional results for leave-one-fold-out feature extraction strategy with TabPFN v2 on regression tasks

To further demonstrate the versatility of our approach, we evaluate TabPFN v2 on regression tasks by extracting embeddings using the leave-one-fold-out strategy and training simple linear regressors on top. As shown in Table 5, our embeddings consistently outperform both vanilla and raw features across different regressors, achieving the best average rank. This result indicates that TabPFN v2 can also serve as an effective feature extractor for regression problems, further supporting its general applicability beyond classification tasks.

Table 5: Average rank comparison of embeddings on regression tasks using different regressors. Lower is better. LR denotes Linear Regression.

| Extraction Strategy | Vanilla | Vanilla | Raw | Raw | Ours | Ours |
|---------------------|----------------|----------------|------|---------|------|---------|
| Regressor | LR | RidgeCV | LR | RidgeCV | LR | RidgeCV |
| Avg. Rank | 5.58 | 5.08 | 3.83 | 3.17 | 2.08 | 1.25 |

C.2 Comparison Between Supervised and Unsupervised Feature Extraction

Our leave-one-fold-out strategy explicitly incorporates label information and accounts for the distinct roles of training and test instances. To further understand the nature of the extracted embeddings, we compare this supervised strategy to two unsupervised alternatives provided by the TabPFN extensions repository.

Let $X \in \mathbb{R}^{n \times d}$ denote a dataset with n samples and d features:

- Unsupervised-Dummy: Each sample is paired with a constant pseudo-target $y = 0 \in \mathbb{R}^n$, forming a regression task. The embedding $E_D \in \mathbb{R}^{n \times h}$ is obtained by extracting the output tokens of the TabPFN regressor.
- Unsupervised-Permute: For each feature $j \in \{1, \dots, d\}$, we treat $\mathbf{x}^{(j)} = X_{:,j}$ as a pseudo-target and use the remaining features $X^{(-j)}$ as input. Depending on the type of $\mathbf{x}^{(j)}$, TabPFN is applied in classification or regression mode to obtain $E^{(j)} \in \mathbb{R}^{n \times h}$. These embeddings are concatenated to a high-dimensional form:

$$E_{P} = \text{concat}(E^{(1)}, E^{(2)}, \dots, E^{(d)}) \in \mathbb{R}^{n \times (d \cdot h)}.$$

We compare these unsupervised methods with our supervised leave-one-fold-out strategy in Table 6. Overall, unsupervised approaches underperform compared to the supervised ones and fail to recover the classification ability of TabPFN v2. This performance gap arises because label information is introduced only post hoc via a linear classifier rather than during embedding extraction. Among the unsupervised methods, the permutation-based approach performs better, likely due to its ability to encode attribute-specific structure.

Figure 6 presents a visual comparison of embeddings produced by the three methods using the same color and marker scheme as in Figure 4. Since unsupervised methods lack label supervision during embedding generation, their embeddings tend to scatter broadly without forming well-separated clusters by class. These results further highlight the contrasting goals of supervised and unsupervised strategies—class separation versus feature distribution coverage, respectively.

C.3 Results for the Non-Partitioned Feature Extraction Variant

Using the same context and query without partitioning, we experimented with a variant where the context contains all training data and the query set includes both training and test points. This

Table 6: Average rank (lower is better) of TabPFN v2 and a linear classifier trained on the extracted embeddings across 29 classification datasets. In addition to the supervised feature extraction strategy considered in the main paper (including the vanilla one, our leave-one-fold-out, and the version based on the combined features), we compare with two *unsupervised* embedding extraction approaches by appending a column of *dummy* labels with zero values and *permuting* each column as labels, respectively.

| \downarrow | TabPFN v2 | Vanilla | Dummy | Permute | Ours | Combined |
|-----------------|----------------|---------|-----------------|---------|--------------|-----------------|
| Rank | 2.66 | 5.72 | 4.90 | 3.69 | 2.16 | 1.88 |
| Accuracy:0.8600 | Accuracy:0.56 | 50 | Accuracy:0.8660 | Acci | uracy:0.8740 | Accuracy:0.9590 |
| Accuracy:0.8876 | Accuracy:0.61 | 05 | Accuracy:0.8843 | Acci | uracy:0.9012 | Accuracy:0.9085 |
| Accuracy:0.5899 | Accuracy: 0.78 | 45 | Accuracy:0.6236 | Acco | uracy:0.7646 | Accuracy:0.8123 |
| Accuracy:0.8782 | Accuracy:0.36 | 90 | Accuracy:0.8266 | Acci | uracy:0.9004 | Accuracy:0.9188 |
| (a) Raw Feature | (b) Vanilla | a | (c) Dummy | (d) | Permute | (e) Ours |

Figure 6: Comparison between unsupervised and supervised (ours) feature extraction. Visualization of extracted embeddings for four datasets: *churn* (first row, two classes), *bank* (second row, two classes), *KDD* (third row, two classes), and *website_phishing* (fourth row, three classes). We use crosses to denote training examples and circles to denote test examples. (a) shows the raw features, while (b) presents the embeddings extracted using the vanilla strategy. (c) and (d) refer to *unsupervised* embedding extraction approaches by appending a column of dummy labels with zero values and permuting each column as labels, respectively. (e) depicts the embeddings obtained using our proposed methods. The accuracy value is calculated by training a linear model (logistic regression) over the extracted embeddings on the training set and predicting on the test set.

non-partitioned strategy improves upon the vanilla feature extraction baseline but still underperforms compared to our proposed leave-one-fold-out method. We attribute this to *role ambiguity*: query points that also appear in the support set (with dummy or ground-truth labels) are treated inconsistently, preventing the network from fully distinguishing between training and test roles and thereby degrading feature consistency.

D Influence of Key Modules and Meta-Feature Analysis

We investigate the influence of two key components in TabPFN v2, *i.e.*, the feature engineering that pre-processes the raw features of a given tabular dataset and the post-hoc ensembleing. In addition, we analyze the conditions under which TabPFN v2 performs well or poorly through a meta-feature-based classification analysis.

Table 7: Performance ranking (lower is better) of different feature extraction strategies on classification tasks. The non-partitioned variant uses the same context and query without data folding.

| Method | Avg. Rank |
|-----------------------------|-----------|
| Leave-one-fold-out (Ours) | 2.10 |
| TabPFN v2 | 2.72 |
| Non-partitioned (12 layers) | 3.07 |
| Non-partitioned (9 layers) | 4.29 |
| Non-partitioned (6 layers) | 4.43 |
| Vanilla (12 layers) | 5.86 |
| Vanilla (9 layers) | 6.62 |
| Vanilla (6 layers) | 6.90 |

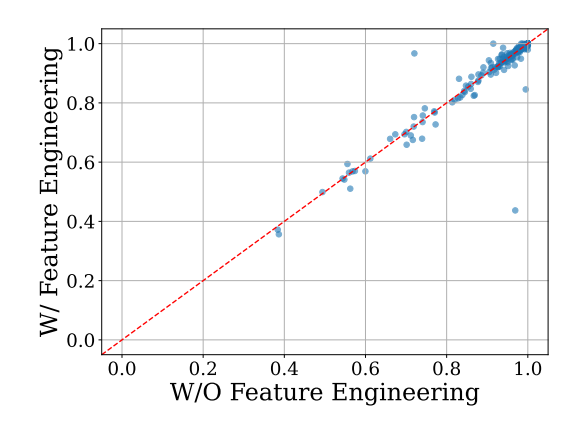


Figure 7: Scatter plot comparing the normalized Accuracy/ R^2 scores. The x-axis represents the normalized Accuracy/ R^2 scores without Feature Engineering, while the y-axis represents the normalized Accuracy/ R^2 scores with Feature Engineering. The red dashed line (y=x) serves as a reference, indicating equal performance.

Feature engineering. TabPFN v2 pre-processes the features of a given tabular dataset with various strategies, such as quantile, category shuffling, SVD, and power transform. Specifically, we examine the effects of adding fingerprint features (add_fingerprint_feature) and polynomial features (polynomial_features) to the raw tabular data. The results indicate that TabPFN v2 performs well even without the use of these engineered features, suggesting that, for the benchmark datasets of [75], these specific feature engineering techniques do not provide a significant improvement. This finding highlights the robustness of TabPFN v2 and its ability to handle raw features effectively, without the need for extensive pre-processing or feature construction. We show the influence of this step in Figure 7.

Model ensemble. Post hoc ensembling (PHE) involves applying TabPFN v2 to the datasets multiple times with different perturbations and aggregating the predictions of these base models at different temperatures. We show the change of performance of TabPFN v2 w.r.t. the number of ensemble numbers (*i.e.*, the number of base models) in Figure 8. On the benchmark of [75], we observe that, overall, ensemble methods improve performance, with larger ensemble sizes yielding better results. However, we also note that even without ensembling, TabPFN v2 performs exceptionally well, and the relative performance gain from ensembling is limited. This suggests that while ensembling can provide further improvements, the base TabPFN v2 model is already highly effective on its own. The equivariant property described in [3] provides insight into this phenomenon. Since TabPFN v2 introduces random tokens to handle heterogeneous features, the model becomes less sensitive to the arbitrary ordering of features, effectively enforcing equivariance in this aspect. As a result, the benefits of ensembling through feature order permutations are less pronounced compared to TabPFN v1.

Meta-Feature Analysis of TabPFN v2 Performance. To better understand the conditions under which TabPFN v2 performs well or poorly, we conducted a meta-learning-based classification analysis using 300 datasets. Specifically, we used the average rank of TabPFN v2 across datasets as a performance indicator. The threshold for classification was set at the mean rank, 6.31. Datasets where

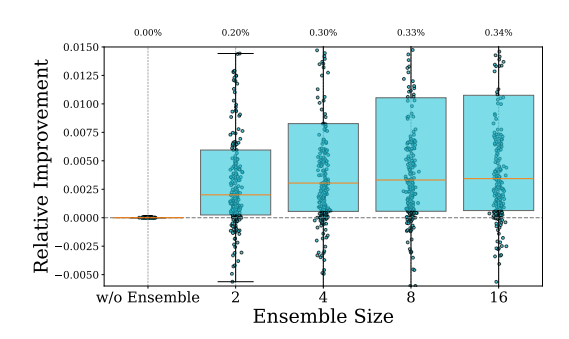


Figure 8: Box plot of relative performance improvements of TabPFN v2 with post hoc ensembling (PHE) across different ensemble sizes (2, 4, 8, and 16 base models). The relative improvement is calculated as the performance gain over the non-ensemble model, where higher values indicate stronger performance. The box plots show the median, interquartile range (IQR), and outliers for each ensemble size.

TabPFN v2 achieved a rank lower than or equal to 6.31 were labeled as "Good", while those with a higher rank were labeled as "Bad". We extracted meta-features from each dataset and used them to train a decision tree classifier, aiming to distinguish between the "Good" and "Bad" categories. All the meta-features utilized in this task are detailed in Table 8, accompanied by their respective explanations. A visual depiction of a simple depth-3 decision tree is shown in Figure 9, and the tree reveals key factors that influence the effectiveness of TabPFN v2. The decision tree visualizes how to predict whether TabPFN v2 performs well ("Good") or poorly ("Bad") on a given dataset, based on dataset meta-features: The root node splits on the number of instances (nr_inst), indicating that TabPFN v2 tends to perform better on datasets with fewer than 24,350 samples. For these smaller datasets, the left subtree further splits on the mean joint entropy (joint_ent.mean), where higher values (greater than 3.028) are associated with improved performance. For datasets with lower mean joint entropy (\leq 3.028), TabPFN v2 also tends to perform well when the number of rows is relatively small (\leq 4,862). In contrast, the right subtree, which represents larger datasets, reveals that a low standard deviation of the interquartile range (iq_range.std) across features (\leq 0.657) is linked to poorer model performance.

E Detailed Results

We list the detailed results of TabPFN v2 and our extensions on various benchmarks.

- We present the **main results of TabPFN v2** on 300 datasets in Table 9. The table includes accuracy for classification tasks and RMSE (Root Mean Squared Error) for regression tasks, along with the corresponding mean and standard deviation for each dataset. Notably, we excluded 27 datasets from these results in Table 9, as they were used by TabPFN v2 to select the best checkpoint. These excluded datasets, which are not shown in Figure 1 (right) and Figure 2 of the main paper, include:
 - (1) ada_prior, allbp, baseball, delta_ailerons, eye_movements, eye_movements_bin, GAMETES_Epistasis_2-Way_20atts_0.1H_EDM-1_1, hill-valley, JapaneseVowels, jungle_chess_2pcs_raw_endgame_complete, led24, longitudinal-survey, page-blocks, ringnorm, rl, thyroid-ann, waveform-5000,
 - (2) debutanizer, delta_elevators, mauna-loa-atmospheric, puma32H, stock_fardamento02, treasury, weather_izmir, wind.
- In Table 10, we showcase the **performance of various models on 18 high-dimensional datasets**. The results display the mean accuracy of different models, including ModernNCA (MNCA), MLP, KNN, RealMLP, XGBoost (XGB), Random Forest (RForest), Logistic Regression (LogReg), and TabPFN v2 (PFN-v2), along with variants like TabPFN v2-pca and TabPFN v2*. This highlights the ability of these models to handle high-dimensional data with many features.
- We demonstrate the **performance of various models on 12 multi-class classification tasks** with more than 10 classes in Table 11. The table provides the mean accuracy of models like KNN, TabPFN-v2*, XGBoost (XGB), CatBoost (CatB), Random Forest (RForest), ModernNCA (MNCA), MLP, Logistic Regression (LogReg), and RealMLP, showcasing how they perform on multi-class tasks with a larger number of classes. Additionally, we compare **PFN-v2-ECOC**, a

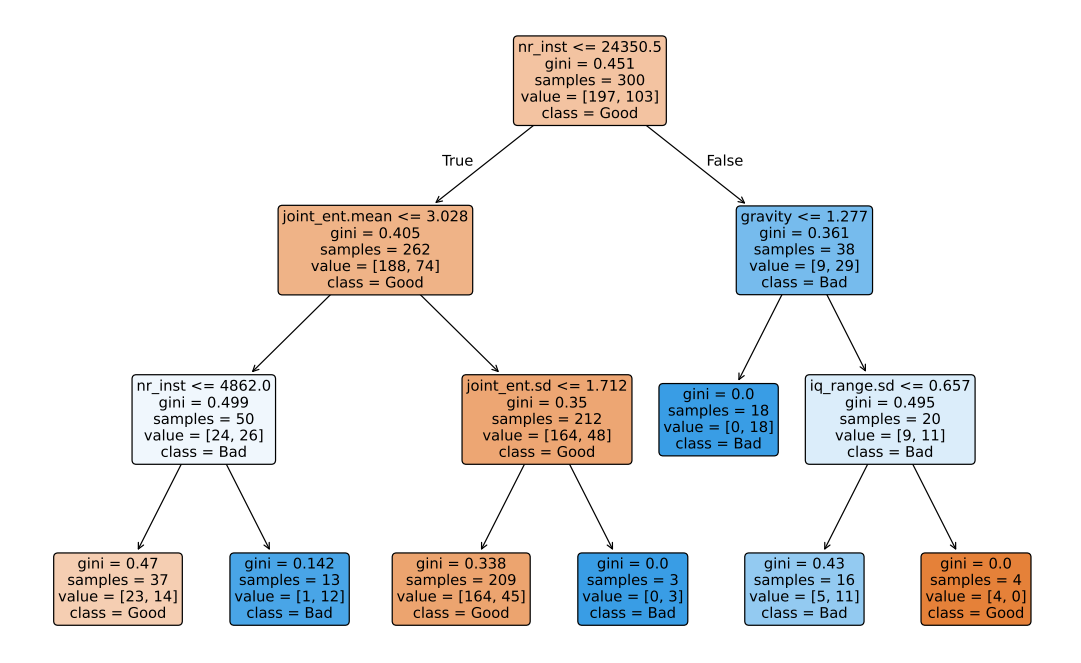


Figure 9: Decision tree for predicting TabPFN v2 performance (Good vs. Bad) based on dataset characteristics, constructed from experiments on 300 datasets. The tree splits on meta-features such as number of instances (nr_inst), joint entropy (joint_ent.mean), number of numerical features (nr_num), distance between minority and majority classes' center of mass (gravity) and interquartile range (iq_range) statistics. Each split is chosen to maximize information gain. The leaf nodes indicate the predicted performance class, the Gini impurity, and class distribution. This tree provides insights into the types of datasets where TabPFN v2 is expected to perform well.

multi-class classification solution provided by [28]. This method extends TabPFN-v2 by leveraging Error-Correcting Output Codes (ECOC) to enhance multi-class classification performance.³

- In Table 12, we compare the **performance of various models on 18 large-scale datasets**. The results show the mean accuracy or RMSE for MLP, Logistic/Linear Regression (LR), KNN, XGBoost (XGB), Random Forest (RForest), CatBoost (CatB), ModernNCA (MNCA), RealMLP, and different versions of TabPFN v2 (PFNv2, PFNv2 with K-means, PFNv2 with Bagging, and PFNv2*). This illustrates the models' performance on large-scale datasets.
- In Table 13, we show the **performance of TabPFN v2 and the extracted feature embeddings** across 29 classification datasets. The table includes average classification accuracy for each dataset when using feature embeddings from different transformer layers (Layer 6, Layer 9, Layer 12), as well as a combined approach where embeddings from multiple layers are concatenated. The "selected layers" column indicates the layers chosen based on validation set performance, offering insights into how different layers contribute to overall model performance. In addition to evaluating the performance of TabPFN v2 and the extracted feature embeddings, we also compared the results with embeddings obtained using the vanilla strategy (Vanilla).

Table 9: Main results of TabPFN v2 on 300 datasets, including accuracy (for classification tasks) and RMSE (for regression tasks), along with the corresponding mean and standard deviation for each dataset. Among the 300 datasets, 200 are classification datasets, and 100 are regression datasets. The results demonstrate the effectiveness of TabPFN v2 across both classification and regression tasks.

| Dataset | Mean + Std | Dataset | Mean + Std |
|-----------------------------|------------------|------------------------|------------------|
| ASP-POTASSCO-classification | 43.50 ± 1.27 | Amazon_employee_access | 94.22 ± 0.04 |
| BLE_RSSI_localization | 73.37 ± 0.15 | BNG(breast-w) | 98.56 ± 0.07 |

³https://github.com/PriorLabs/tabpfn-community/blob/main/src/tabpfn_extensions/many_class/many_class_classifier.py

| BNG(circa) | | | | |
|---|-------------------------------------|------------------|----------------------------------|------------------|
| Cationsi-Housing-Classification 91.47 ± 0.17 Cardiovasculur-Disease-dataset 72.92 ± 0.13 Contaminant-10.5GHz 93.17 ± 0.03 Contaminant-10.0GHz 93.93 ± 0.50 Contaminant-10.5GHz 93.11 ± 0.47 Contaminant-10.0GHz 93.93 ± 0.50 Contaminant-10.5GHz 93.11 ± 0.47 Contaminant-10.0GHz 93.93 ± 0.50 Contaminant-10.5GHz 93.11 ± 0.47 Contaminant-9.5GHz 93.93 ± 0.50 FOREX_Belinopathy_Debreven 93.84 ± 0.07 Employee 48.80 ± 0.07 FOREX_Budded-day-High 74.51 ± 0.51 FOREX_anded-hour-High 71.01 ± 0.20 FOREX_anded-day-High 74.51 ± 0.51 FOREX_anded-hour-High 71.01 ± 0.20 FOREX_anded-bour-High 74.51 ± 0.51 FOREX_anded-hour-High 69.77 ± 0.48 FOREX_Candiby-hour-High 70.55 ± 0.49 FOREX_anded-hour-High 69.77 ± 0.48 FOREX_Candiby-hour-High 70.55 ± 0.49 FOREX_anded-hour-High 69.81 ± 0.39 FOREX_Candiby-hour-High 70.55 ± 0.49 FOREX_anded-hour-High 69.81 ± 0.39 FOREX_Candiby-hour-High 70.55 ± 0.49 FOREX_anded-hour-High 69.81 ± 0.39 FOREX_Candiby-hour-High 70.55 ± 0.49 FOREX_anded-hour-High 70.81 ± 0.49 FOREX_Candiby-hour-High 70.55 ± 0.49 FOREX_anded-hour-High 69.81 ± 0.39 FOREX_Candiby-hour-High 70.55 ± 0.49 FOREX_anded-hour-High 70.81 ± 0.49 FOREX_Candiby-hour-High 70.81 ± 0.51 Fore-Toronome 70.81 ± 0.49 FOREX_Candiby-hour-High 70.81 ± 0.49 Fore-Toronome 70.81 ± 0.49 FOREX_Candiby-hour-High 70.81 ± 0.49 Fore-Toronome 70.81 ± 0.49 | BNG(cmc) | 57.69 ± 0.17 | BNG(tic-tac-toe) | 79.42 ± 0.26 |
| Citcle, prediction, small | Bank_Customer_Churn_Dataset | 87.53 ± 0.12 | Basketball_c | 70.65 ± 0.47 |
| Citcle, prediction, small | California-Housing-Classification | 91.47 ± 0.17 | Cardiovascular-Disease-dataset | 72.92 ± 0.13 |
| Contaminam-1-1.0GHz | | | | |
| Contaminana-9-3GHz | | | I . | |
| Credit_C | | | | |
| Dalabeits Retinopathy Debrecon | | | | |
| Employee | | | | |
| FOREX_auded-day-High | Diabetic_Retinopathy_Debrecen | 72.81 ± 1.07 | E-CommereShippingData | 67.54 ± 0.21 |
| FOREX_audisp\-chay-High | Employee | 84.80 ± 0.30 | FICO-HELOC-cleaned | 75.35 ± 0.21 |
| FOREX_audisp\-chay-High | FOREX audcad-day-High | 74.51 ± 0.51 | FOREX audcad-hour-High | 71.01 ± 0.20 |
| FOREX_audipy-hour-High | | | | |
| FOREX_adips/-bour-High | | | | |
| FOREX_cadipy-hour-ligh | | | | |
| Fitness_Club_c | | | | 71.68 ± 0.53 |
| GAMETES, Heterogeneity 65.90 ± 1.84 Heart-Disease-Dataset 10123 ± 0.54 Heart-Disease-Dataset 10124 ± 0.23 Heart-Disease-Dataset 10125 ± 0.64 Heart-Disease-Dataset 10124 ± 0.03 Heterschinal-Bias-Assessment 1026 ± 0.05 Herschinal-Bias-Assessment 1026 ± 0.05 Herschinal-Bias-Assessment 1026 ± 0.05 Herschinal-Bias-Assessment 1026 ± 0.05 Herschinal-Bias-Assessment 1027 ± 0.05 Herschinal-Bias-Assessment 1027 ± 0.05 Herschinal-Bias-Assessment 1028 ± 0.05 Herschinal-B | FOREX_cadjpy-hour-High | 70.55 ± 0.40 | Firm-Teacher-Direction | 84.42 ± 0.47 |
| GesturePhaseSegmentationProcessed | Fitness_Club_c | 79.67 ± 0.24 | GAMETES_Epistasis | 68.75 ± 0.82 |
| GesturePhaseSegmentationProcessed | GAMETES Heterogeneity | 65.90 ± 1.84 | Gender Gap in Spanish WP | 60.58 ± 0.24 |
| Heart-Disease-Dataset | | | | |
| Indian_pines | 2 | | | |
| Intersectional-Bias-Assessment 94.73 ± 0.13 Is-this-a-good-customer 88.41 ± 0.04 Agances/owels 99.68 ± 0.08 KDD RDDCup09_upselling 81.06 ± 0.26 Long 99.88 ± 0.00 MIC 90.20 ± 0.56 Magic felescope 88.13 ± 0.21 Mobile_Price_Classification 97.10 ± 0.29 Prishing Websites 96.74 ± 0.13 PricChard 87.31 ± 0.28 Prima_Indians_Diabetes_Database 75.93 ± 0.06 Pricchard 87.31 ± 0.28 Priza_Rutter3 88.20 ± 0.45 Spring_Indians_Diabetes_Database 75.93 ± 0.06 Priza_Rutter3 88.20 ± 0.45 Spring_Indians_Database 97.33 ± 0.06 Spring_Indians_Database 97.33 ± 0.07 Spring_Indians_Database 97.34 ± 0.25 Spring_Database 97.34 ± 0.25 Spring | | | | |
| Japances/owels 99.68 ± 0.08 KDD SDD 99.88 ± 0.00 MIC 90.20 ± 0.56 Magic felescope 88.13 ± 0.21 Morkiteing. Campaign 88.11 ± 0.41 Mobile_Price_Classification 97.10 ± 0.29 Prichard 87.21 ± 0.22 Prichard 87.31 ± 0.28 Prima_Indians_Diabetes_Database 75.93 ± 0.66 PizzaCutter3 88.20 ± 0.45 Prima_Indians_Diabetes_Database 75.93 ± 0.66 PizzaCutter3 97.33 ± 0.06 PizzaCutter3 97.33 ± 0.06 PizzaCutter3 97.33 ± 0.06 PizzaCutter3 98.95 ± 0.00 PizzaCutter3 Prima_Indians_Databates 98.95 ± 0.00 PizzaCutter3 Prima_Indians_Databates 98.95 ± 0.00 PizzaCutter3 Prima_Indians_Databates PizzaCutter3 | | | | |
| MIC | | | | |
| MIC 90.20 ± 0.56 Magic Telescope 88.13 ± 0.21 Nutrition Health, Survey 83.45 ± 0.22 Performance-Prediction 73.23 ± 0.61 Phishing Websites 96.74 ± 0.13 87.31 ± 0.28 Pima Indians, Diabetes_Database 75.93 ± 0.66 PizzaCutter3 88.20 ± 0.45 Pumpkin Seeds 87.93 ± 0.66 PizzaCutter3 88.50 ± 0.50 Shipping 68.73 ± 0.40 SDSS17 97.33 ± 0.06 Shipping 68.73 ± 0.40 SDSS17 97.33 ± 0.06 Waler_Quality_and_Potability 65.49 ± 0.50 Waterstress 95.18 ± 0.50 Will 99.28 ± 0.06 accelerometer 37.96 ± 1.32 ada ada 85.54 ± 0.25 adal, agnostic 38.99 ± 0.34 adult 88.99 ± 0.12 airlines_2000 62.28 ± 0.48 allibp 97.85 ± 0.19 airlines_2000 62.28 ± 0.48 allrep auto-ui-at-2500 69.81 ± 1.00 auto-ui-ar-2110 41.18 ± 1.58 bank 9.02 ± 0.22 auto-ui-ar-2110 41.18 ± 1.58 bank 9.05 ± 0.28 auto-ui-ar-2110 <td>JapaneseVowels</td> <td>99.68 ± 0.08</td> <td>KDD</td> <td>80.14 ± 0.46</td> | JapaneseVowels | 99.68 ± 0.08 | KDD | 80.14 ± 0.46 |
| MIC 90.20 ± 0.56 Magic Telescope 88.13 ± 0.21 Nutrition Health, Survey 83.45 ± 0.22 Performance-Prediction 73.23 ± 0.61 Phishing Websites 96.74 ± 0.13 87.31 ± 0.28 Pima Indians, Diabetes_Database 75.93 ± 0.66 PizzaCutter3 88.20 ± 0.45 Pumpkin Seeds 87.93 ± 0.66 PizzaCutter3 88.50 ± 0.50 Shipping 68.73 ± 0.40 SDSS17 97.33 ± 0.06 Shipping 68.73 ± 0.40 SDSS17 97.33 ± 0.06 Waler_Quality_and_Potability 65.49 ± 0.50 Waterstress 95.18 ± 0.50 Will 99.28 ± 0.06 accelerometer 37.96 ± 1.32 ada ada 85.54 ± 0.25 adal, agnostic 38.99 ± 0.34 adult 88.99 ± 0.12 airlines_2000 62.28 ± 0.48 allibp 97.85 ± 0.19 airlines_2000 62.28 ± 0.48 allrep auto-ui-at-2500 69.81 ± 1.00 auto-ui-ar-2110 41.18 ± 1.58 bank 9.02 ± 0.22 auto-ui-ar-2110 41.18 ± 1.58 bank 9.05 ± 0.28 auto-ui-ar-2110 <td>KDDCup09 upselling</td> <td>81.06 ± 0.26</td> <td>Long</td> <td>99.88 ± 0.00</td> | KDDCup09 upselling | 81.06 ± 0.26 | Long | 99.88 ± 0.00 |
| Marketing_Campaign 88.11 ± 0.41 Mobile_Price_Classification 97.10 ± 0.29 Nutrition_Health_Survey 34.5 ± 0.21 Performance-Prediction 73.23 ± 0.61 Pinia_Indians_Diabetes_Database 75.93 ± 0.61 Picchart3 87.31 ± 0.28 Pinia_Indians_Diabetes_Database 75.93 ± 0.21 QSAR_biodegradation 88.50 ± 0.50 Rain_in_Australia 38.88 ± 0.11 76.84 0.50 Shipping 68.73 ± 0.40 Telecom_Chum_Dataset 95.18 ± 0.50 UII_Pen_Characters 45.71 ± 2.16 ValkoneVul 98.95 ± 0.00 Water_Quality_and_Potability 65.49 ± 0.50 Waterstress 71.37 ± 0.96 Wilt 99.23 ± 0.06 abolone 63.58 ± 0.38 ada_apostic 38.39 ± 0.34 ada_prior 62.28 ± 0.48 albo 38.99 ± 0.34 ada_prior 62.28 ± 0.48 allbp 97.85 ± 0.19 altrep 98.65 ± 0.12 autoUniv-au4-2500 69.81 ± 1.00 also to | | 90.20 ± 0.56 | MagicTelescope | 88.13 ± 0.21 |
| Nutrition_Health_Survey | | | | |
| PhishingWebsites 96.74 ± 0.13 PicCharr3 87.31 ± 0.28 Pumpkin Seeds 87.93 ± 0.66 PizzaCutter3 88.50 ± 0.04 Stock Pumpkin Seeds 87.93 ± 0.21 SDSS17 97.33 ± 0.06 PizzaCutter3 88.50 ± 0.05 Pumpkin Seeds Rain in Australia 83.88 ± 0.11 SDSS17 97.33 ± 0.06 Shipping 68.73 ± 0.40 UIL Pen_Characters 45.71 ± 2.16 VulNoneVul 98.95 ± 0.00 VulNoneVul 99.95 ± 0.00 VulNoneVul 99.95 ± 0.00 VulNoneVul 99.95 ± 0.00 VulNoneVul 99.95 ± 0.00 VulNoneVul | | | | |
| Pima Indiams, Diabetes Database 75,93 ± 0.66 PizzaCutter3 88.20 ± 0.45 Numpkin, Seeds 87.93 ± 0.21 OSAR_biodegradation 88.50 ± 0.45 OSAR_biodegradation 99.18 ± 0.50 OSAR_biodegradation 99.51 ± 0.30 OSAR_biod | | | | |
| Rain jn Australia 83.88 ± 0.11 SDSS17 97.33 ± 0.06 | | | | |
| Rain in _Australia | Pima_Indians_Diabetes_Database | 75.93 ± 0.66 | PizzaCutter3 | 88.20 ± 0.45 |
| Shipping | Pumpkin_Seeds | 87.93 ± 0.21 | QSAR_biodegradation | 88.50 ± 0.50 |
| Shipping | Rain in Australia | 83.88 ± 0.11 | SDSS17 | 97.33 ± 0.06 |
| UII Pen_Characters | | 68.73 ± 0.40 | | 95.18 ± 0.50 |
| Water Quality and Potability 65.49 ± 0.50 Waterstress 71.37 ± 0.96 Wilf 99.28 ± 0.06 abalone 63.58 ± 0.38 accelerometer 73.96 ± 1.32 ada 85.40 ± 0.25 add, agnostic 83.99 ± 0.34 ada prior 85.32 ± 0.19 adult 85.93 ± 0.12 airlines, 2000 62.28 ± 0.48 allby analcatdata, authorship 99.72 ± 0.29 artificial-characters 73.90 ± 0.99 analcatdata, authorship 99.72 ± 0.29 artificial-characters 73.90 ± 0.99 bank 90.86 ± 0.19 bank note, authentication 55.64 ± 0.18 baseball 93.81 ± 0.40 car-evaluation 95.56 ± 0.18 company, bankruptcy_prediction 97.33 ± 0.07 compass 71.05 ± 0.29 connect-4 76.78 ± 0.35 contraceptive_method_choice 62.10 ± 0.37 credit 78.10 ± 0.11 credit-g 79.50 ± 0.81 default_of_credit_card_clients 82.63 ± 0.08 delta_ailerons 95.47 ± 0.09 drug_consumption 40.32 ± 0.00 delta_ailerons 95.75 ± 0.20 | | | | |
| Wilt 99.28 ± 0.06 abalone 63.58 ± 0.38 accelerometer 73.96 ± 1.32 ada 85.40 ± 0.25 ada agnostic 83.99 ± 0.34 ada prior 85.32 ± 0.19 allthe 97.85 ± 0.12 airlines 2000 62.28 ± 0.48 allthe 99.72 ± 0.29 autioUniv-au-1100 41.18 ± 1.58 bank 90.86 ± 0.19 bank houte authentication 55.64 ± 0.18 baseball 93.81 ± 0.40 car-evaluation 59.59 ± 0.22 company-bankruptcy-prediction 97.33 ± 0.07 compass 71.05 ± 0.22 comnect-4 76.78 ± 0.35 contraceptive_method_choice 62.10 ± 0.37 credit 78.10 ± 0.11 delteses_130-us_bospitals 63.08 ± 0.07 dis 90.07 ± 0.14 dan 97.25 ± 0.20 drug_consumption 40.32 ± 0.00 delta_ailerons 95.47 ± 0.09 deg_e-g-vestate 98.34 ± 0.12 euclerticity 86.57 ± 0.10 eeg_e-g-vestate 98.34 ± 0.12 euclerticity 86.57 ± 0.10 eogpovements 77.03 ± 1.68 eye_movements_bi | | | | |
| accelerometer 73.96 ± 1.32 ada 85.40 ± 0.25 ada_gnostic 83.99 ± 0.34 ada_prior 85.32 ± 0.19 adult 85.93 ± 0.12 airlines 2000 62.28 ± 0.48 allbp 97.85 ± 0.19 allrep 98.65 ± 0.12 analcatdata_authorship 99.72 ± 0.29 atiricial-characters 73.90 ± 0.99 autoUniv-au-4-2500 69.81 ± 1.00 bank 90.86 ± 0.19 bank 99.86 ± 0.19 bank note_authentication 55.64 ± 0.18 baseball 93.81 ± 0.40 care-valuation 98.29 ± 0.22 chum 96.33 ± 0.28 company_bankruptcy_prediction cm 59.59 ± 0.49 connect-4 76.78 ± 0.35 contraceptive_method_choice 62.10 ± 0.37 credit 7.78.10 ± 0.31 dabetes_130-us_hospitals 63.08 ± 0.07 discustomer_satisfaction_in_aritine 94.79 ± 0.11 dabetes_130-us_hospitals 63.08 ± 0.07 dirug_consumption 40.32 ± 0.00 dry_bean_dataset 92.76 ± 0.10 drug_consumption 40.32 ± 0.00 dry_bean_dataset 92.76 ± 0.10 | | | I . | |
| ada_ agnostic 83.99 ± 0.34 ada_prior 85.32 ± 0.19 adult 85.93 ± 0.12 airlines_2000 62.28 ± 0.48 allbp 97.85 ± 0.19 alfree 98.65 ± 0.12 analcatdat_authorship 99.72 ± 0.29 artificial-characters 73.90 ± 0.99 bank 90.86 ± 0.19 banknote_authentication 55.64 ± 0.18 baseball 93.81 ± 0.40 car-evaluation 98.29 ± 0.22 cump 20.33 ± 0.28 cmc 59.59 ± 0.49 company_bankruptcy_prediction 97.33 ± 0.07 compass 71.05 ± 0.29 connect-4 76.78 ± 0.35 contraceptive_method_choice 62.10 ± 0.37 credit 78.10 ± 0.11 credit-g 79.50 ± 0.81 dis 99.07 ± 0.14 dna 97.25 ± 0.20 drug_consumption 40.32 ± 0.00 dry_bean_dataset 92.76 ± 0.10 ege-ge-state 98.36 ± 0.24 euclyptus 82.63 ± 0.18 eye_movements 77.03 ± 1.68 eye_movements_bin 67.28 ± 2.60 first-order-theorem-proving 61.12 ± 0.70 ga-drift | | | abalone | |
| adult 85.93 ± 0.12 airlines 2000 62.28 ± 0.48 allbp 97.85 ± 0.19 allrep 98.65 ± 0.12 analcatdata_authorship 99.72 ± 0.29 artificial-characters 73.90 ± 0.99 autoUniv-au+2500 69.81 ± 1.00 autoUniv-au7-1100 41.88 ± 1.58 baseball 93.81 ± 0.40 car-evaluation 98.29 ± 0.22 churn 96.33 ± 0.28 cmc 59.59 ± 0.49 company_bankruptcy_prediction 97.33 ± 0.07 compass 71.05 ± 0.29 connect-4 76.78 ± 0.35 contraceptive_method_choice 62.10 ± 0.37 credit 27.67 ± 0.01 dabetes_130-us_hospitals 63.08 ± 0.07 default_of_credit_card_clients 82.63 ± 0.08 delta_ailerons 95.47 ± 0.09 drug_consumption 40.32 ± 0.00 dry_bean_dataset 97.25 ± 0.20 drug_consumption 40.32 ± 0.00 dry_bean_dataset 92.76 ± 0.45 estimation_of_obesity_levels 98.66 ± 0.24 eucalyptus 72.88 ± 1.17 ey_movements 77.03 ± 1.68 ey_movements_bin 67.28 ± 2.60 fi | accelerometer | 73.96 ± 1.32 | ada | 85.40 ± 0.25 |
| allbp | ada_agnostic | 83.99 ± 0.34 | ada_prior | 85.32 ± 0.19 |
| allbp | adult | 85.93 ± 0.12 | airlines 2000 | 62.28 ± 0.48 |
| analcatdata_authorship 99.72 ± 0.29 artificial-characters 73.90 ± 0.99 autoUniv-au4-2500 69.81 ± 1.00 autoUniv-au7-1100 41.18 ± 1.58 baseball 93.81 ± 0.40 car-evaluation 55.64 ± 0.18 chum 96.33 ± 0.28 cmc 59.59 ± 0.49 company_bankruptcy_prediction 97.33 ± 0.07 compass 71.05 ± 0.29 connect-4 76.78 ± 0.35 contraceptive_method_choice 62.10 ± 0.37 credit 76.78 ± 0.35 contraceptive_method_choice 62.10 ± 0.37 credit 76.78 ± 0.35 contraceptive_method_choice 62.10 ± 0.37 credit 62.01 ± 0.37 credit_g 79.50 ± 0.81 default_of_credit_eard_clients 82.63 ± 0.08 delta_ailerons 95.47 ± 0.09 dis 99.07 ± 0.14 dna 97.25 ± 0.20 drug_consumption 40.32 ± 0.00 dry_bean_dataset 92.76 ± 0.10 cege_ye-state 98.34 ± 0.12 electricity 86.57 ± 0.45 estimation_of_obesity_levels 98.66 ± 0.24 eucalyptus 72.88 ± 1.17 coff_play_d | | | _ | |
| autoUniv-au4-2500 69.81 ± 1.00 bank 20.86 ± 0.19 bank 20.86 ± 0.19 bankhote_authentication 55.64 ± 0.18 baseball 33.81 ± 0.40 car-evaluation 98.29 ± 0.22 chum 96.33 ± 0.28 cmc 59.59 ± 0.49 car-evaluation 98.29 ± 0.22 cmc car-evaluation 98.29 ± 0.28 cmc car-evaluation 98.29 ± 0.28 cmc car-evaluation 98.29 ± 0.28 | | | | |
| base ball 90.86 ± 0.19 banknote_authentication 55.64 ± 0.18 baseball 93.81 ± 0.40 car-evaluation 98.29 ± 0.22 churn 96.33 ± 0.28 cmc 59.59 ± 0.49 company_bankruptcy_prediction 97.33 ± 0.07 compass 71.05 ± 0.29 contraceptive_method_choice 62.10 ± 0.37 credit 78.10 ± 0.11 credit_g 79.50 ± 0.81 customer_satisfaction_in_airline 94.79 ± 0.11 dabetes_130-us_hospitals 63.08 ± 0.07 default_of_credit_card_clients 82.63 ± 0.08 delta_ailerons 95.47 ± 0.09 dis 99.07 ± 0.14 dna 97.25 ± 0.20 drug_consumption 40.32 ± 0.00 dry_bean_dataset 92.76 ± 0.10 drug_consumption 61.24 ± 0.12 dry_bean_da | | | | |
| baseball churm 93.81 ± 0.40 car-evaluation 98.29 ± 0.22 cumm 96.33 ± 0.28 cm cm 55.95 ± 0.49 company_bankruptcy_prediction 97.33 ± 0.07 company_bankruptcy_prediction 75.95 ± 0.49 connect-4 76.78 ± 0.35 contraceptive_method_choice 62.10 ± 0.37 credit 78.10 ± 0.11 credit_g 79.50 ± 0.81 customer_satisfaction_in_airline 94.79 ± 0.11 dabetes_130-us_hospitals 63.08 ± 0.07 dis 99.07 ± 0.14 dna 97.25 ± 0.20 drug_consumption 40.32 ± 0.00 delta_ailerons 95.47 ± 0.09 drug_consumption 40.32 ± 0.00 dry_bean_dataset 92.76 ± 0.10 eeg-ey-state 98.66 ± 0.24 eucalyptus 72.88 ± 1.17 eye_movements 77.03 ± 1.68 eye_movements_bin 67.28 ± 2.60 first-order-theorem-proving 61.12 ± 0.70 gas-drift 99.47 ± 0.04 polus_IbH_adataset_extended 92.60 ± 0.44 helena 33.32 ± 0.21 heloc 72.75 ± 0.20 hill-valley 98.33 ± 0.52 | | | | |
| chum 96.33 ± 0.28 cmc 59.59 ± 0.49 company_bankruptcy_prediction 97.33 ± 0.07 compas 71.05 ± 0.29 connect-4 76.78 ± 0.35 contraceptive_method_choice 62.10 ± 0.37 credit 78.10 ± 0.11 credit-g 79.50 ± 0.81 customer_satisfaction_in_airline 94.79 ± 0.11 dabetes_130-us_hospitals 63.08 ± 0.07 default_of_credit_card_clients 82.63 ± 0.08 delta_ailerons 95.47 ± 0.09 dis 99.07 ± 0.14 dna 97.25 ± 0.20 drug_consumption 40.32 ± 0.00 dry_bean_dataset 92.76 ± 0.10 eeg-eye-state 98.34 ± 0.12 electricity 86.57 ± 0.45 estimation_of_obesity_levels 98.66 ± 0.24 eucalyptus 72.88 ± 1.17 eye_movements 77.03 ± 1.68 eye_movements_bin 67.28 ± 2.60 first-order-theorem-proving 61.12 ± 0.70 gas-drift 99.47 ± 0.04 poll_play_dataset_extended 92.60 ± 0.44 helena 33.32 ± 0.21 heloc 72.75 ± 0.20 hinternet_inewall 92.85 ± 0.20 i | bank | 90.86 ± 0.19 | banknote_authentication | 55.64 ± 0.18 |
| company_bankruptcy_prediction 97.33 ± 0.07 compass 71.05 ± 0.29 condect-4 76.78 ± 0.35 contraceptive_method_choice 62.10 ± 0.37 credit 78.10 ± 0.11 credit:g 79.50 ± 0.81 customer_satisfaction_in_airline 94.79 ± 0.11 dabetes_130-us_hospitals 63.08 ± 0.07 default_of_credit_card_clients 82.63 ± 0.08 delta_ailerons 95.47 ± 0.09 dis 99.07 ± 0.14 dna 97.25 ± 0.20 drug_consumption 40.32 ± 0.00 delta_ailerons 95.47 ± 0.09 ceg-eye-state 98.34 ± 0.12 electricity 86.57 ± 0.10 eeg-eye-state 98.66 ± 0.24 eucalyptus 72.88 ± 1.17 eye_movements 77.03 ± 1.68 eye_movements bin 67.28 ± 2.60 first-order-theorem-proving 61.12 ± 0.70 gas-drift 99.47 ± 0.04 golf_play_dataset_extended 92.60 ± 0.44 helena 33.32 ± 0.21 heloc 72.75 ± 0.20 hill-valley 98.33 ± 0.52 louse_16H 88.55 ± 0.38 htru htru 97.95 ± 0.06 | baseball | 93.81 ± 0.40 | car-evaluation | 98.29 ± 0.22 |
| company_bankruptcy_prediction 97.33 ± 0.07 compass 71.05 ± 0.29 connect-4 76.78 ± 0.35 contraceptive_method_choice 62.10 ± 0.37 credit 78.10 ± 0.11 credit:g 79.50 ± 0.81 default_of_credit_card_clients 82.63 ± 0.08 delta_ailerons 95.47 ± 0.09 dis 99.07 ± 0.14 delta_ailerons 95.47 ± 0.09 drug_consumption 40.32 ± 0.00 drug_bean_dataset 92.76 ± 0.10 ceg-eye-state 98.34 ± 0.12 electricity 86.57 ± 0.10 eeg-eye-state 98.66 ± 0.24 eucalyptus 72.88 ± 1.17 eye_movements 77.03 ± 1.68 eye_movements bin 67.28 ± 2.60 forst-order-theorem-proving 61.12 ± 0.70 gas-drift 99.47 ± 0.04 golf_play_dataset_extended 92.60 ± 0.44 belena 33.32 ± 0.21 heloc 72.75 ± 0.20 bill-valley 98.33 ± 0.52 blum-employee-performance 100.0 ± 0.00 in_vehicle_coupon 73.29 ± 0.06 internet_trewall 92.85 ± 0.30 internet_usage 54.34 ± 2.64 | churn | 96.33 ± 0.28 | cmc | 59.59 ± 0.49 |
| $\begin{array}{c} \text{connect-4} \\ \text{credit} \\ \text{credit} \\ \text{credit} \\ \text{credit} \\ \text{credit} \\ \text{customer_satisfaction_in_airline} \\ \text{default_of_credit_card_clients} \\ \text{dis} \\ \text{dis} \\ \text{dis} \\ \text{drug_consumption} \\ \text{du}, 32 \pm 0.08 \\ \text{drug_consumption} \\ \text{du}, 32 \pm 0.00 \\ \text{dry_bean_dataset} \\ \text{get_cricity} \\ \text{ges_consumption} \\ \text{du}, 32 \pm 0.00 \\ \text{dry_bean_dataset} \\ \text{get_cricity} \\ \text{ges_consumption} \\ \text{ges_consumption} \\ \text{du}, 32 \pm 0.00 \\ \text{dry_bean_dataset} \\ \text{get_cricity} \\ \text{ges_consumption} \\ ges_consumptio$ | company bankruptcy prediction | 97.33 ± 0.07 | compass | 71.05 ± 0.29 |
| $ \begin{array}{c} \text{credit} \\ \text{customer_satisfaction_in_airline} \\ \text{default_of_credit_card_clients} \\ \text{des} \\ 2.63 \pm 0.08 \\ \text{dis} \\ \text{op.} \\ \text{drug_consumption} \\ \text{eeg-eye-state} \\ \text{eeg-eye-state} \\ \text{estimation_of_obesity_levels} \\ \text{estimation_of_obesity_levels} \\ \text{estimation_of_obesity_levels} \\ \text{estimation_of_obesity_levels} \\ \text{ep.} \\ 3.4 \pm 0.12 \\ \text{eve_movements} \\ \text{77.03 \pm 1.68} \\ \text{eye_movements} \\ \text{forts-order-theorem-proving} \\ \text{fol.} \\ 1.2 \pm 0.70 \\ \text{golf_play_dataset_extended} \\ \text{pol.} \\ \text{play_dataset_extended} \\ \text{plous_dataset_extended} \\ \text{plous_dataset_dataset} \\ plous_data$ | | | | |
| customer_satisfaction_in_airline 94,79 ± 0.11 dabetes_130-us_hospitals 63.08 ± 0.07 defaul_of_credit_card_clients 82.63 ± 0.08 delta_ailerons 95.47 ± 0.09 dis 99.07 ± 0.14 dna 97.25 ± 0.20 drug_consumption 40.32 ± 0.00 dry_bean_dataset 92.76 ± 0.10 eeg-eye-state 98.34 ± 0.12 electricity 86.57 ± 0.45 estimation_of_obesity_levels 98.66 ± 0.24 eucalyptus 72.88 ± 1.17 eye_movements 77.03 ± 1.68 eye_movements_bin 67.28 ± 2.60 first-order-theorem-proving 61.12 ± 0.70 gas-drift 99.47 ± 0.04 golf_play_dataset_extended 92.60 ± 0.44 helena 33.32 ± 0.21 heloc 72.75 ± 0.20 hill-valley 98.33 ± 0.52 house_16H 88.55 ± 0.18 htru 97.95 ± 0.06 ibm-employee-performance 100.0 ± 0.00 in_vehicle_coupon 73.20 ± 0.35 internet_trievall 92.85 ± 0.30 internet_usage 54.34 ± 2.64 jamine 81.34 ± 0.42 jml 81.32 ± 0.10 jungle | | | | |
| $\begin{array}{cccccccccccccccccccccccccccccccccccc$ | | | | |
| $\begin{array}{llllllllllllllllllllllllllllllllllll$ | | | | |
| drug_consumption 40.32 ± 0.00 dry_bean_dataset 92.76 ± 0.10 eeg-eye-state 98.34 ± 0.12 electricity 86.57 ± 0.45 estimation_of_obesity_levels 98.66 ± 0.24 eucalyptus 72.88 ± 1.17 eye_movements 77.03 ± 1.68 eye_movements_bin 67.28 ± 2.60 first-order-theorem-proving 61.12 ± 0.70 gas-drift 99.47 ± 0.04 golf_play_dataset_extended 92.60 ± 0.44 helena 33.32 ± 0.21 heloc 72.75 ± 0.20 hill-valley 98.33 ± 0.52 house_16H 88.855 ± 0.18 htru 97.95 ± 0.06 ibm-employee-performance 100.0 ± 0.00 in_vehicle_coupon 73.20 ± 0.35 internet_frewall 92.85 ± 0.30 internet_usage 54.34 ± 2.64 jasmine 81.34 ± 0.42 jml 81.32 ± 0.10 jungle_chess_2pcs_raw_endgame 85.97 ± 1.82 kcl 86.65 ± 0.34 kd_ipums_la_97-small 88.50 ± 0.12 kr-vs-k 78.46 ± 1.01 kr-vs-kp 99.64 ± 0.15 kropt 77.96 ± 0.63 law-school-admission-bianry | default_of_credit_card_clients | 82.63 ± 0.08 | delta_ailerons | 95.47 ± 0.09 |
| eeg-eye-state 98.34 ± 0.12 electricity 86.57 ± 0.45 estimation_of_obesity_levels 98.66 ± 0.24 eucalyptus 72.88 ± 1.17 eye_movements 77.03 ± 1.68 eye_movements_bin 67.28 ± 2.60 first-order-theorem-proving of first-order-theorem-proving of play_dataset_extended 92.60 ± 0.44 helena 33.32 ± 0.21 heloc 72.75 ± 0.20 hill-valley 98.33 ± 0.52 house_16H 88.55 ± 0.18 htru 97.95 ± 0.06 ibm-employee-performance 100.0 ± 0.00 in_ehicle_coupon 73.20 ± 0.35 internet_firewall 92.85 ± 0.30 internet_usage 54.34 ± 2.64 jumingle_chess_2pcs_raw_endgame 85.97 ± 1.82 kcl 86.65 ± 0.34 kdd_ipums_la_97-small 88.50 ± 0.12 kr-vs-k 78.46 ± 1.01 kdv-y-skp 99.64 ± 0.15 kropt 77.96 ± 0.63 law-school-admission-bianry 100.0 ± 0.00 led24 73.29 ± 0.62 led7 73.99 ± 0.31 letter 97.57 ± 0.10 madeline 90.72 ± 0.48 mammography 98.71 ± 0.05 | dis | 99.07 ± 0.14 | dna | 97.25 ± 0.20 |
| eeg-eye-state 98.34 ± 0.12 electricity 86.57 ± 0.45 estimation_of_obesity_levels 98.66 ± 0.24 eucalyptus 72.88 ± 1.17 eye_movements 77.03 ± 1.68 eye_movements_bin 67.28 ± 2.60 first-order-theorem-proving of first-order-theorem-proving of play_dataset_extended 92.60 ± 0.44 helena 33.32 ± 0.21 heloc 72.75 ± 0.20 hill-valley 98.33 ± 0.52 house_16H 88.55 ± 0.18 htru 97.95 ± 0.06 ibm-employee-performance 100.0 ± 0.00 in_ehicle_coupon 73.20 ± 0.35 internet_firewall 92.85 ± 0.30 internet_usage 54.34 ± 2.64 jumingle_chess_2pcs_raw_endgame 85.97 ± 1.82 kcl 86.65 ± 0.34 kdd_ipums_la_97-small 88.50 ± 0.12 kr-vs-k 78.46 ± 1.01 kdv-y-skp 99.64 ± 0.15 kropt 77.96 ± 0.63 law-school-admission-bianry 100.0 ± 0.00 led24 73.29 ± 0.62 led7 73.99 ± 0.31 letter 97.57 ± 0.10 madeline 90.72 ± 0.48 mammography 98.71 ± 0.05 | drug consumption | 40.32 ± 0.00 | dry bean dataset | 92.76 ± 0.10 |
| estimation_of_obesity_levels eye_movements 77.03 ± 1.68 eye_movements 77.03 ± 1.68 eye_movements 67.28 ± 2.60 first-order-theorem-proving golf_play_dataset_extended 92.60 ± 0.44 helena 33.32 ± 0.21 heloc 72.75 ± 0.20 hill-valley 98.33 ± 0.52 house_16H 88.55 ± 0.18 htru 97.95 ± 0.06 him-employee-performance 100.0 ± 0.00 in_vehicle_coupon 73.20 ± 0.35 internet_firewall 92.85 ± 0.30 internet_usage 54.34 ± 2.64 jasmine 81.34 ± 0.42 jml jungle_chess_2pcs_raw_endgame 85.97 ± 1.82 kcl 86.65 ± 0.34 kdd_ipums_la_97-small 88.50 ± 0.12 kr-vs-kp 99.64 ± 0.15 kropt 100.0 ± 0.00 led24 73.29 ± 0.62 led7 73.99 ± 0.31 letter 97.57 ± 0.10 madeline 90.72 ± 0.48 mammography 98.71 ± 0.05 maternal_health_risk 83.28 ± 0.64 mfeat-fourier 89.85 ± 0.86 mfeat-factors 96.98 ± 0.28 mfeat-zernike 84.10 ± 0.87 mice_protein_expression 100.0 ± 0.00 microaggregation2 62.80 ± 0.14 mozilla4 93.58 ± 0.16 national-longitudinal-survey-binary one-hundred-plants-margin 88.56 ± 0.74 one-hundred-plants-texture 90.94 ± 0.75 one-hundred-plants-texture 90.95 ± 0.26 ozone_level 97.86 ± 0.11 page-blocks 97.67 ± 0.16 page-blocks 97.67 ± 0.13 page-blocks 97.67 ± 0.16 page-blocks 97.67 ± 0.18 page- | | 98.34 ± 0.12 | | |
| $ \begin{array}{c} \text{eye_movements} & 77.03 \pm 1.68 \\ \text{first-order-theorem-proving} & 61.12 \pm 0.70 \\ \text{golf_play_dataset_extended} & 92.60 \pm 0.44 \\ \text{helco} & 72.75 \pm 0.20 \\ \text{house_16H} & 88.55 \pm 0.18 \\ \text{ibm-employee-performance} & 100.0 \pm 0.00 \\ \text{imternet_firewall} & 92.85 \pm 0.30 \\ \text{jasmine} & 81.34 \pm 0.42 \\ \text{jamine} & 88.50 \pm 0.12 \\ \text{kdd_ipums_la_97-small} & 88.50 \pm 0.12 \\ \text{kr-vs-kp} & 99.64 \pm 0.15 \\ \text{ked7} & 73.99 \pm 0.31 \\ \text{led7} & 73.99 \pm 0.31 \\ \text{led8} & 90.72 \pm 0.48 \\ \text{mfeat-fourier} & 89.85 \pm 0.86 \\ \text{mfeat-morphological} & 83.28 \pm 0.64 \\ \text{mfeat-morphological} & 76.63 \pm 0.50 \\ \text{mfeat-zernike} & 84.10 \pm 0.87 \\ \text{morital-longitudinal-survey-binary} & 100.0 \pm 0.00 \\ \text{more-londerd-plants-texture} & 90.94 \pm 0.75 \\ \text{opol_londer} & 97.86 \pm 0.11 \\ \text{pol_long} & 98.87 \pm 0.36 \\ \text{pol_long} & 98.80 \pm 0.09 \\ \text{pol_long} & 98.80 \pm 0.09 \\ \text{predict_students_dropout} & 78.14 \pm 0.38 \\ \text{pol_long} & 99.56 \pm 0.16 \\ \text{pol_long} & 98.80 \pm 0.09 \\ \text{predict_students_dropout} & 78.11 \pm 0.38 \\ \text{pol_long} & 99.56 \pm 0.06 \\ \text{predict_students_dropout} & 78.11 \pm 0.38 \\ \text{pol_long} & 98.80 \pm 0.09 \\ \text{predict_students_dropout} & 78.11 \pm 0.38 \\ \text{pol_long} & 98.81 \pm 0.38 \\ \text{predict_students_dropout} & 78.11 \pm 0.38 \\ \text{pol_long} & 98.80 \pm 0.09 \\ \text{predict_students_dropout} & 78.11 \pm 0.38 \\ \text{pol_long} & 98.80 \pm 0.09 \\ \text{predict_students_dropout} & 78.11 \pm 0.38 \\ \text{pol_long} & 98.80 \pm 0.09 \\ \text{predict_students_dropout} & 78.11 \pm 0.38 \\ \text{pol_long} & 98.80 \pm 0.09 \\ \text{predict_students_dropout} & 78.11 \pm 0.38 \\ \text{pol_long} & 98.80 \pm 0.09 \\ \text{predict_students_dropout} & 78.11 \pm 0.38 \\ \text{pol_long} & 99.56 \pm 0.16 \\ \text{pol_long} & 98.80 \pm 0.09 \\ \text{predict_students_dropout} & 78.11 \pm 0.38 \\ \text{pol_long} & 99.56 \pm 0.06 \\ \text{pol_long} & 98.80 \pm 0.09 \\ \text{predict_students_dropout} & 78.11 \pm 0.38 \\ \text{pol_long} & 99.56 \pm 0.06 \\ \text{pol_long} & 98.80 \pm 0.09 \\ \text{predict_students_dropout} & 78.11 \pm 0.38 \\ \text{pol_long} & 99.56 \pm 0.06 \\ \text{pol_long} & 98.80 \pm 0.09 \\ \text{predict_students_dropout} & 78.11 \pm 0.38 \\ \text{pol_long} & 99.56 \pm 0.06 \\ \text{pol_long} & 98.8$ | | | | |
| $\begin{array}{llllllllllllllllllllllllllllllllllll$ | | | | |
| $\begin{array}{cccccccccccccccccccccccccccccccccccc$ | 3 — | | | |
| heloc 72.75 ± 0.20 hill-valley 98.33 ± 0.52 house_16H 88.55 ± 0.18 htru 97.95 ± 0.06 ibm-employee-performance 100.0 ± 0.00 in_vehicle_coupon 73.20 ± 0.35 internet_firewall 92.85 ± 0.30 internet_usage 54.34 ± 2.64 jasmine 81.34 ± 0.42 jm1 81.32 ± 0.10 jungle_chess_2pcs_raw_endgame 85.97 ± 1.82 kc1 86.65 ± 0.34 kdd_ipums_la_97-small 88.50 ± 0.12 kr-vs-k 78.46 ± 1.01 kr-vs-kp 99.64 ± 0.15 kropt 77.96 ± 0.63 law-school-admission-bianry 100.0 ± 0.00 led24 73.29 ± 0.62 led7 73.99 ± 0.31 letter 97.57 ± 0.10 madeline 90.72 ± 0.48 mamography 98.71 ± 0.05 maternal_health_risk 83.28 ± 0.64 mfeat-factors 96.98 ± 0.28 mfeat-morphological 76.63 ± 0.50 mfeat-karhunen 96.42 ± 0.24 mfeat-greation2 62.80 ± 0.14 microaggregation2 62.80 ± 0.14 mobile_c36_oversampling | | | 1 5 | |
| house_16H 88.55 ± 0.18 ibm-employee-performance htru 97.95 ± 0.06 in_vehicle_coupon 73.20 ± 0.35 internet_firewall 92.85 ± 0.30 internet_usage 54.34 ± 2.64 ± 2.64 jml 81.32 ± 0.10 jmgle_chess_2pcs_raw_endgame 81.34 ± 0.42 jml 81.32 ± 0.10 jmgle_chess_2pcs_raw_endgame 85.97 ± 1.82 kcl kcl 86.65 ± 0.34 kdd_ipums_la_97-small 88.50 ± 0.12 kr-vs-k 78.46 ± 1.01 kr-vs-kp 99.64 ± 0.15 kropt 77.96 ± 0.63 law-school-admission-bianry 100.0 ± 0.00 led24 73.29 ± 0.62 led7 73.99 ± 0.31 letter 90.72 ± 0.48 mammography 98.71 ± 0.05 maternal_health_risk 83.28 ± 0.64 mfeat-factors 96.98 ± 0.28 mfeat-factors 96.98 ± 0.28 mfeat-factors 96.98 ± 0.28 mfeat-factors 96.98 ± 0.28 mfeat-pixel 96.10 ± 0.32 mfeat-pixel 96.10 ± 0.00 mfeat-pixel 96.10 ± 0.00 mfeat-pixel 96.10 ± 0.00 mfeat-pixel 96.10 | | | I . | |
| $\begin{array}{cccccccccccccccccccccccccccccccccccc$ | heloc | 72.75 ± 0.20 | hill-valley | 98.33 ± 0.52 |
| $\begin{array}{cccccccccccccccccccccccccccccccccccc$ | house_16H | 88.55 ± 0.18 | htru | 97.95 ± 0.06 |
| $\begin{array}{llllllllllllllllllllllllllllllllllll$ | | | in_vehicle_coupon | |
| $\begin{array}{cccccccccccccccccccccccccccccccccccc$ | | 92.85 ± 0.30 | | 54.34 ± 2.64 |
| $ \begin{array}{cccccccccccccccccccccccccccccccccccc$ | | | | |
| $\begin{array}{cccccccccccccccccccccccccccccccccccc$ | | | 1 2 | |
| $\begin{array}{cccccccccccccccccccccccccccccccccccc$ | | | | |
| $ \begin{array}{c ccccccccccccccccccccccccccccccccccc$ | -1 | | | |
| $ \begin{array}{llllllllllllllllllllllllllllllllllll$ | | | | |
| $\begin{array}{cccccccccccccccccccccccccccccccccccc$ | law-school-admission-bianry | 100.0 ± 0.00 | led24 | 73.29 ± 0.62 |
| $\begin{array}{cccccccccccccccccccccccccccccccccccc$ | led7 | 73.99 ± 0.31 | letter | 97.57 ± 0.10 |
| $\begin{array}{cccccccccccccccccccccccccccccccccccc$ | madeline | 90.72 ± 0.48 | mammography | 98.71 ± 0.05 |
| $\begin{array}{cccccccccccccccccccccccccccccccccccc$ | | | | |
| $\begin{array}{cccccccccccccccccccccccccccccccccccc$ | | | | |
| $\begin{array}{cccccccccccccccccccccccccccccccccccc$ | | | I . | |
| $\begin{array}{cccccccccccccccccccccccccccccccccccc$ | | | | |
| $\begin{array}{cccccccccccccccccccccccccccccccccccc$ | | | | |
| $\begin{array}{cccccccccccccccccccccccccccccccccccc$ | | | | |
| $\begin{array}{cccccccccccccccccccccccccccccccccccc$ | mozilla4 | 93.58 ± 0.16 | naticusdroid+android+permissions | 96.41 ± 0.10 |
| $\begin{array}{cccccccccccccccccccccccccccccccccccc$ | national-longitudinal-survey-binary | 100.0 ± 0.00 | okcupid_stem | 74.47 ± 0.12 |
| $\begin{array}{cccccccccccccccccccccccccccccccccccc$ | | | | |
| $ \begin{array}{cccccccccccccccccccccccccccccccccccc$ | | | | |
| $ \begin{array}{cccccccccccccccccccccccccccccccccccc$ | | | | |
| $\begin{array}{cccccccccccccccccccccccccccccccccccc$ | | | | |
| $ \begin{array}{cccccccccccccccccccccccccccccccccccc$ | | | | |
| $ \begin{array}{cccccccccccccccccccccccccccccccccccc$ | | | | |
| $ \begin{array}{cccccccccccccccccccccccccccccccccccc$ | pc4 | 90.87 ± 0.36 | pendigits | 99.56 ± 0.06 |
| pol 98.80 \pm 0.09 predict_students_dropout 78.11 \pm 0.38 | philippine | | | 88.47 ± 0.35 |
| | | | | |
| 72 ± 5.25 Illigation 70.00 ± 0.15 | | | | |
| | | /2 ± 0.25 | | 70.00 ± 0.13 |

| | 0604 1 0 44 | | 02.20 0.20 |
|---|--------------------------------------|---------------------------------------|--------------------------------------|
| rl segment | 86.04 ± 0.44 93.91 ± 0.19 | satimage seismic+bumps | 92.30 ± 0.29 93.40 ± 0.08 |
| segment semeion | 93.91 ± 0.19 92.41 ± 0.94 | shill-bidding | 90.31 ± 0.18 |
| shrutime | 86.97 ± 0.11 | shuttle | 99.86 ± 0.04 |
| spambase | 94.85 ± 0.19 | splice | 96.61 ± 0.22 |
| sports_articles | 84.93 ± 0.40 | statlog | 72.13 ± 0.97 |
| steel_plates_faults | 84.68 ± 0.55 | svmguide3 | 85.54 ± 0.54 |
| sylvine | 97.30 ± 0.27 | taiwanese_bankruptcy_prediction | 97.20 ± 0.07 |
| telco-customer-churn | 80.29 ± 0.28 | texture | 100.0 ± 0.00 |
| W thyroid | 99.48 ± 0.06 | thyroid-ann | 99.34 ± 0.08 |
| thyroid-dis | 68.75 ± 0.34 | turiye_student_evaluation | 51.74 ± 0.18 |
| twonorm | 97.94 ± 0.08 | vehicle | 84.31 ± 1.29 |
| walking-activity | 61.22 ± 0.22 | wall-robot-navigation | 99.44 ± 0.10 |
| water quality | 90.12 ± 0.12 | waveform-5000 | 86.29 ± 0.26 |
| waveform_v1 | 86.59 ± 0.25 | website_phishing | 90.48 ± 0.48 |
| wine | 75.12 ± 0.72 | wine-quality-red | 58.35 ± 0.76 |
| wine-quality-white | 64.15 ± 0.69 | yeast | 60.18 ± 0.65 |
| 1000-Cameras-Dataset | 607.71 ± 6.61 | 2dplanes | 1.01 ± 0.00 |
| RSSI_Estimation | 0.00068 ± 0.00 | RSSI_Estimation1 | 0.00092 ± 0.00 |
| Abalone_reg | 2.08 ± 0.00 | Ailerons | 0.00015 ± 0.00 |
| Fiat | 716.20 ± 4.05 | BNG(echoMonths) | 11.41 ± 0.03 |
| BNG(lowbwt) | 455.27 ± 0.78 | BNG(mv) | 4.63 ± 0.01 |
| BNG(stock) | 2.95 ± 0.02 | Bias_correction_r | 0.60 ± 0.01 |
| Bias_correction_r_2 | 0.52 ± 0.01 | Brazilian_houses_reproduced | 0.01 ± 0.00 |
| CPMP-2015-regression | 478.02 ± 5.40 | CPS1988 | 364.02 ± 0.24 |
| CookbookReviews | 1.52 ± 0.02 | Data_Science_Salaries | 60237.28 ± 102.97 |
| Diamonds | 533.30 ± 6.30 | Facebook_Comment_Volume | 23.16 ± 0.20 |
| Food_Delivery_Time | 7.55 ± 0.03 | Goodreads-Computer-Books | 0.43 ± 0.00 |
| IEEE80211aa-GATS | 0.02 ± 0.00 | Job_Profitability | 13.14 ± 0.02 |
| bike_sharing_demand | 68.41 ± 0.60 | Laptop_Prices_Dataset | 439.87 ± 3.10 |
| Wave_Energy_Perth_100 | 15507.90 ± 104.31 | Wave_Energy_Sydney_100 | 14737.67 ± 150.43 |
| Wave_Energy_Sydney_49 | 4567.97 ± 64.02 | MIP-2016-regression | 20966.10 ± 454.90 |
| MiamiHousing2016 | 83101.09 ± 507.30 | Mobile_Phone_Market | 714.87 ± 11.15 |
| Moneyball | 19.42 ± 0.08 | NASA_PHM2008 | 40.24 ± 0.06 |
| NHANES_age_prediction | 15.47 ± 0.04 | OnlineNewsPopularity | 8606.54 ± 7.04 |
| Parkinson_Sound_Record | 14.58 ± 0.09 | Parkinsons_Telemonitoring | 0.60 ± 0.04 |
| Physicochemical_r | 3.45 ± 0.04 | SAT11-HAND-runtime | 1232.03 ± 58.01 |
| Shop_Customer_Data | 28.56 ± 0.01 | Superconductivty | 10.17 ± 0.07 |
| Wine_Quality_red | 0.65 ± 0.00 | Wine_Quality_white | 0.68 ± 0.00 |
| airfoil_self_noise | 1.16 ± 0.02 | analcatdata_supreme | 0.09 ± 0.00 |
| archive2 | 342.64 ± 3.20 | archive_r56_Portuguese | 2.86 ± 0.02 |
| auction_verification | 1145.54 ± 146.94 | avocado_sales | 0.09 ± 0.00 |
| bank32nh | 0.08 ± 0.00 | bank8FM | 0.03 ± 0.00 |
| boston | 4.25 ± 0.19 | chscase_foot | 0.95 ± 0.00 |
| colleges | 0.14 ± 0.00 | combined_cycle_power_plant | 3.22 ± 0.05 |
| communities_and_crime | 0.13 ± 0.00 | concrete_compressive_strength | 4.63 ± 0.07 |
| cpu_act | 2.65 ± 0.03 | cpu_small | 3.06 ± 0.02 |
| dataset_sales delta_elevators | 4.04 ± 0.02 | debutanizer elevators | 0.04 ± 0.00 |
| fifa | 0.0014 ± 0.00 0.78 ± 0.00 | fried | 0.0019 ± 0.00 1.01 ± 0.00 |
| garments worker productivity | 0.78 ± 0.00 0.13 ± 0.00 | gas_turbine_emission | 0.44 ± 0.00 |
| healthcare_insurance_expenses | 4716.87 ± 36.52 | house_16H_reg | 29631.75 ± 251.56 |
| house_8L | 28617.41 ± 202.41 | house_ron_reg house_prices_nominal | 30676.02 ± 2455.4 |
| house_sales_reduced | 132655.03 ± 1847.33 | houses | 42559.98 ± 928.78 |
| | 1009361.62 ± 8758.05 | kin8nm | 0.08 ± 0.00 |
| housing_price_prediction mauna-loa-atmospheric-co2 | 0.39 ± 0.01 | mv | 0.03 ± 0.00 0.02 ± 0.00 |
| pol_reg | 3.84 ± 0.10 | pole | 3.21 ± 0.14 |
| puma32H | 0.01 ± 0.00 | puma8NH | 3.21 ± 0.14 3.24 ± 0.00 |
| qsar_aquatic_toxicity | 1.05 ± 0.01 | qsar_fish_toxicity | 0.86 ± 0.01 |
| satellite_image | 0.65 ± 0.00 | sensory | 0.77 ± 0.01 |
| socmob | 19.53 ± 0.64 | space_ga | 0.09 ± 0.00 |
| steel_industry_energy | 0.37 ± 0.03 | stock | 0.65 ± 0.00 0.65 ± 0.01 |
| stock_fardamento02 | 17.57 ± 0.08 | sulfur | 0.03 ± 0.01 0.03 ± 0.00 |
| topo 2 1 | 0.03 ± 0.00 | treasury | 0.23 ± 0.00 |
| | | volume | 52.09 ± 0.34 |
| us crime | 0.14 ± 0.00 | Volume | J4.07 I 0.34 |
| us_crime weather_izmir | 0.14 ± 0.00 1.09 ± 0.01 | wind | 2.83 ± 0.00 |

F Limitations

While this paper does not introduce a new model architecture or training paradigm, it offers a timely and principled analysis of TabPFN v2, a powerful tabular foundation model. Our contributions lie in empirically evaluating its strengths, identifying its limitations, and proposing practical extensions that enhance its applicability—particularly to large-scale, high-dimensional, and multi-class settings. A key limitation of our work is that the proposed extensions are primarily post-hoc and do not fully

Table 8: Meta-features used in the meta-feature analysis of TabPFN v2 performance.

| Meta-Feature | Explanation |
|----------------|---|
| attr_conc | The concentration coef. of each pair of distinct attributes. |
| class_conc | The concentration coefficient between each attribute and class. |
| class_ent | The target attribute Shannon's entropy. |
| inst_to_attr | The ratio between the number of instances and attributes. |
| mean | The mean value of each attribute. |
| sd | The standard deviation of each attribute. |
| var | The variance of each attribute. |
| range | The range (max - min) of each attribute. |
| iq_range | The interquartile range (IQR) of each attribute. |
| nr_attr | The total number of attributes. |
| sparsity | The (possibly normalized) sparsity metric for each attribute. |
| t_mean | The trimmed mean of each attribute. |
| nr_bin | The number of binary attributes. |
| nr_cat | The number of categorical attributes. |
| nr_num | The number of numeric features. |
| nr_norm | The number of attributes normally distributed based in a given method. |
| nr_cor_attr | The number of distinct highly correlated pair of attributes. |
| gravity | The distance between minority and majority classes' center of mass. |
| nr_class | The number of distinct classes. |
| joint_ent | The joint entropy between each attribute and class. |
| attr_ent | Shannon's entropy for each predictive attribute. |
| cov | The absolute value of the covariance of distinct dataset attribute pairs. |
| eigenvalues | The eigenvalues of covariance matrix from dataset. |
| eq_num_attr | The number of attributes equivalent for a predictive task. |
| max | The maximum value from each attribute. |
| min | The minimum value from each attribute. |
| median | The median value from each attribute. |
| freq_class | The relative frequency of each distinct class. |
| mad | The Median Absolute Deviation (MAD) adjusted by a factor. |
| mad | The Median Absolute Deviation (MAD) adjusted by a factor. |
| mut_inf | The mutual information between each attribute and target. |
| nr_inst | The number of instances (rows) in the dataset. |
| nr_outliers | The number of attributes with at least one outlier value. |
| ns_ratio | The noisiness of attributes. |
| imblance_ratio | The ratio of the number of instances in the minority to the majority class. |
| attr_to_inst | The ratio between the number of attributes. |

address the scalability constraints inherent to the original architecture. Nevertheless, by improving model usability without retraining, we reduce the computational and environmental costs typically associated with large model development.

To the best of our knowledge, this work poses no explicit ethical concerns. It provides practical guidance for applying pre-trained tabular models in real-world domains such as healthcare and finance, where transparency and efficiency are essential. Our study highlights the value of understanding and extending foundation models alongside architectural innovation.

Table 10: Performance of various models on 18 high-dimensional datasets. The results show the mean accuracy of different models, including ModernNCA (MNCA), MLP, KNN, RealMLP, XGBoost (XGB), Random Forest (RForest), Logistic Regression (LogReg), TabPFN v2 (PFN-v2), TabPFN v2 with PCA (v2-pca), TabPFN v2 with subsampling (v2*), ProtoGate (ProtoG), and CatBoost (CatB). The performance is evaluated on high-dimensional datasets, with the values representing mean accuracy for each model.

| Dataset | MNCA | MLP | KNN | RealMLP | XGB | RForest | LogReg | PFN-v2 | v2-pca | v2* | ProtoG | CatB |
|-------------|-------|-------|-------|---------|-------|---------|--------|--------|--------|-------|--------|-------|
| CLL_SUB_111 | 62.90 | 72.46 | 57.39 | 70.43 | 73.04 | 70.14 | 73.91 | 70.14 | 57.68 | 71.59 | 65.51 | 71.59 |
| BASEHOCK | 96.31 | 97.01 | 71.88 | 97.46 | 95.29 | 96.73 | 96.99 | 69.09 | 97.41 | 97.36 | 96.32 | 95.87 |
| Prostate_GE | 81.27 | 86.98 | 80.00 | 87.94 | 89.52 | 87.94 | 91.43 | 95.24 | 88.57 | 94.29 | 84.13 | 94.92 |
| PCMAC | 88.21 | 88.53 | 66.48 | 90.15 | 91.64 | 92.20 | 87.15 | 92.70 | 90.76 | 90.14 | 88.21 | 92.01 |
| GLI_85 | 81.57 | 85.49 | 76.47 | 89.80 | 82.35 | 83.92 | 90.59 | 80.39 | 86.27 | 92.55 | 81.96 | 80.78 |
| RELATHE | 88.18 | 90.54 | 75.03 | 90.23 | 87.11 | 87.30 | 90.49 | 86.36 | 87.65 | 89.95 | 89.92 | 90.35 |
| SMK_CAN_187 | 63.51 | 66.84 | 69.47 | 69.82 | 66.49 | 70.70 | 72.11 | 71.05 | 71.75 | 72.10 | 70.71 | 71.40 |
| warpPIE10P | 98.41 | 99.05 | 92.38 | 100.0 | 94.92 | 98.57 | 100.0 | 100.0 | 100.0 | 100.0 | 97.79 | 98.89 |
| leukemia | 90.22 | 95.11 | 86.67 | 94.67 | 97.78 | 92.00 | 96.00 | 92.44 | 93.33 | 96.00 | 94.00 | 94.22 |
| orlraws10P | 97.67 | 98.33 | 92.00 | 99.00 | 84.33 | 99.00 | 99.00 | 92.00 | 99.33 | 99.67 | 92.67 | 99.00 |
| GLIOMA | 58.00 | 60.67 | 68.00 | 67.33 | 66.67 | 64.00 | 64.00 | 62.67 | 69.33 | 68.67 | 69.91 | 66.67 |
| warpAR10P | 83.08 | 85.64 | 53.08 | 97.44 | 81.28 | 87.18 | 97.69 | 90.77 | 95.38 | 96.67 | 90.04 | 87.44 |
| TOX_171 | 76.00 | 88.19 | 70.86 | 90.48 | 78.10 | 78.67 | 90.29 | 80.95 | 82.48 | 87.24 | 85.52 | 83.05 |
| lung | 91.54 | 95.45 | 93.66 | 95.28 | 93.66 | 92.68 | 95.12 | 95.28 | 93.50 | 95.61 | 95.43 | 93.01 |
| ALLAML | 87.56 | 95.56 | 81.33 | 96.89 | 96.00 | 96.44 | 92.00 | 92.89 | 93.78 | 94.67 | 91.14 | 94.67 |
| colon | 78.46 | 78.97 | 76.92 | 83.08 | 74.87 | 82.56 | 86.15 | 81.54 | 78.46 | 79.49 | 78.46 | 77.95 |
| gisette | 97.21 | 97.57 | 95.04 | 97.86 | 97.55 | 96.82 | 97.51 | 97.35 | 97.26 | 97.23 | 97.18 | 97.78 |
| arcene | 81.67 | 85.50 | 84.50 | 81.00 | 75.00 | 86.83 | 88.00 | 83.67 | 88.33 | 92.00 | 85.33 | 85.00 |
| Mean | 82.86 | 87.11 | 77.29 | 88.83 | 84.76 | 86.87 | 89.36 | 85.25 | 87.29 | 89.73 | 86.37 | 87.48 |

Table 11: Performance of various models on 12 multi-class classification tasks with more than 10 classes. The results show the mean accuracy of different models, including KNN, PFN-v2*, PFN-v2-ECOC, XGB (XGBoost), CatBoost (CatB), Random Forest (RForest), ModernNCA (MNCA), Multi-layer Perceptron (MLP), Logistic Regression (LogReg), and RealMLP. The performance is evaluated on 12 multi-class datasets with more than 10 classes, with accuracy values presented for each model on the respective datasets.

| Dataset | KNN | PFN-v2* | PFN-v2-DPT | PFN-v2-ECOC | XGB | CatB | RForest | MNCA | MLP | LogReg | RealMLP |
|--------------------|-------|---------|------------|-------------|-------|-------|---------|-------|-------|--------|---------|
| 100-plants-texture | 79.69 | 90.94 | 82.67 | 84.92 | 77.06 | 89.73 | 82.65 | 80.52 | 83.92 | 86.88 | 88.35 |
| 100-plants-margin | 77.50 | 88.56 | 81.94 | 79.40 | 74.25 | 84.06 | 82.79 | 77.60 | 80.44 | 79.69 | 83.58 |
| 100-plants-shape | 60.31 | 79.52 | 72.15 | 63.38 | 56.15 | 65.19 | 64.33 | 70.10 | 47.33 | 65.94 | 72.08 |
| UJI_Pen_Characters | 36.26 | 45.71 | 33.38 | 44.20 | 30.35 | 38.88 | 34.24 | 44.03 | 37.75 | 19.41 | 46.37 |
| texture | 98.45 | 100.0 | 99.98 | 100.0 | 98.55 | 99.13 | 96.76 | 99.68 | 99.40 | 99.64 | 99.95 |
| letter | 94.90 | 97.57 | 96.69 | 97.78 | 96.26 | 96.75 | 91.56 | 97.96 | 96.40 | 75.80 | 98.31 |
| walking-activity | 60.29 | 61.22 | 57.28 | 61.92 | 65.06 | 64.92 | 61.74 | 64.85 | 60.64 | 27.02 | 65.13 |
| helena | 28.94 | 33.31 | 28.54 | 19.20 | 32.42 | 37.90 | 33.91 | 36.58 | 37.91 | 33.40 | 38.55 |
| internet_usage | 30.17 | 54.34 | 50.51 | 50.86 | 51.08 | 37.90 | 33.91 | 52.09 | 43.00 | 37.73 | 52.23 |
| kropt | 71.22 | 77.96 | 71.44 | 77.11 | 86.95 | 79.26 | 71.77 | 78.27 | 64.45 | 28.08 | 92.03 |
| kr-vs-k | 70.78 | 78.46 | 71.54 | 76.29 | 87.26 | 74.81 | 71.60 | 76.83 | 65.03 | 28.03 | 91.85 |
| ASP-POTASSCO | 34.75 | 43.50 | 41.88 | 45.27 | 42.24 | 41.08 | 42.86 | 37.45 | 29.63 | 35.14 | 41.70 |
| Mean | 61.94 | 70.93 | 65.67 | 66.69 | 66.47 | 67.47 | 64.01 | 68.00 | 62.16 | 51.40 | 72.51 |

Table 12: Performance of various models on 18 large-scale datasets. The results show the mean accuracy/RMSE of different models, including MLP, Logistic Regression/Linear Regression (LR), KNN, XGBoost (XGB), Random Forest (RForest), CatBoost (CatB), ModernNCA (MNCA), RealMLP, and various versions of TabPFN v2: original TabPFN v2 (PFNv2), TabPFN v2 with K-means (PFNv2-K), TabPFN v2 with Bagging (PFNv2-B), PFNv2* (TabPFNv2*), PFNv2-DT (TabPFN-DT), and PFNv2-DF (TabPFN-DF).

| Dataset | MLP | LR | KNN | XGB | RForest | CatB | MNCA | RealMLP | PFNv2 | PFNv2-K | PFNv2-B | PFNv2* | PFNv2-DT | PFNv2-DF |
|--------------------------------|-------|----------|-------|-------|---------|-------|-------|---------|-------|---------|---------|--------|----------|----------|
| BNG(credit-a) | 90.07 | 85.98 | 87.41 | 90.21 | 89.25 | 91.13 | 89.98 | 90.91 | 89.55 | 89.01 | 89.66 | 89.89 | 90.45 | 90.43 |
| CDC_Indicators | 86.79 | 86.55 | 86.39 | 86.76 | 86.60 | 86.78 | 86.76 | 86.76 | 86.65 | 86.68 | 86.69 | 86.74 | 86.75 | 86.70 |
| Higgs | 75.53 | 64.29 | 65.16 | 73.33 | 71.87 | 74.81 | 73.28 | 75.36 | 71.64 | 71.56 | 72.01 | 72.13 | 73.53 | 73.62 |
| Smoking_signal | 73.90 | 72.53 | 72.36 | 73.87 | 73.08 | 73.99 | 73.63 | 74.00 | 73.47 | 73.37 | 73.55 | 73.69 | 73.74 | 73.84 |
| nomao | 96.19 | 94.59 | 95.20 | 96.92 | 96.07 | 97.03 | 96.68 | 96.37 | 96.08 | 96.29 | 96.12 | 96.18 | 96.75 | 96.34 |
| sf-police-incidents | 87.84 | 87.84 | 85.87 | 87.68 | 87.84 | 87.87 | - | 87.84 | 87.84 | 87.84 | 87.84 | 87.84 | 87.84 | 87.84 |
| Data_Crowdfunding | 96.48 | 67.04 | 93.70 | 96.89 | 95.29 | 96.81 | 96.53 | 96.71 | 94.59 | 91.81 | 94.96 | 95.07 | 96.90 | 96.83 |
| Fashion-MNIST | 89.54 | 85.69 | 86.00 | 90.03 | 86.57 | 90.24 | 89.36 | 90.25 | 68.40 | 82.82 | 83.89 | 86.26 | 78.91 | 78.82 |
| covertype | 94.01 | 72.54 | 92.76 | 96.30 | 78.30 | 90.77 | 97.31 | 97.38 | 83.54 | 82.95 | 84.16 | 86.85 | 97.38 | 97.44 |
| jannis | 71.99 | 64.60 | 65.67 | 71.83 | 69.19 | 72.26 | 72.57 | 73.00 | 70.24 | 70.26 | 70.59 | 71.31 | 72.57 | 72.50 |
| poker-hand | 99.99 | 50.12 | 54.01 | 99.51 | 64.63 | 97.69 | 76.31 | 99.88 | 41.97 | 38.86 | 36.80 | 54.12 | 91.13 | 92.33 |
| volkert | 69.85 | 58.75 | 67.41 | 69.74 | 62.71 | 70.88 | 77.18 | 73.76 | 62.82 | 62.15 | 62.81 | 64.84 | 68.66 | 67.76 |
| Airlines_DepDelay (×101) | 2.905 | 2.933 | 3.170 | 2.891 | 2.907 | 2.881 | - | 2.482 | 2.937 | 2.933 | 2.937 | 2.915 | 2.900 | 2.897 |
| Wave_Energy_Farm (×103) | 8.199 | 13.19 | 32.29 | 6.917 | 7.294 | 7.173 | 6.148 | 59.05 | 7.214 | 8.375 | 7.063 | 10.506 | 6.616 | 6.785 |
| UJIndoorLoc (×100) | 9.958 | ∞ | 9.004 | 10.47 | 23.19 | 9.139 | 5.990 | 65.34 | 66.49 | 7.825 | 7.435 | 9.538 | 14.404 | 7.472 |
| blogfeedback (×101) | 2.387 | ∞ | 2.410 | 2.093 | 2.026 | 2.044 | 1.953 | 2.105 | 3.073 | 2.687 | 2.700 | 2.014 | 1.914 | 1.944 |
| microsoft ($\times 10^{-1}$) | 7.577 | 7.782 | 8.284 | 7.514 | 7.566 | 7.453 | 7.573 | 5.077 | 7.735 | 7.981 | 7.720 | 7.612 | 7.944 | 7.728 |
| yahoo (×10 ⁻¹) | 7.692 | 7.997 | 8.504 | 7.629 | - | 7.514 | - | 5.671 | 8.148 | 8.332 | 8.132 | 7.961 | 16.409 | 8.069 |

Table 13: Performance of TabPFN v2 and the extracted feature embeddings across 29 classification datasets. The table shows the average classification accuracy for each dataset when using different layers (Layer 6, Layer 9, Layer 12) of the transformer as feature embeddings, as well as the "combined" approach, where embeddings from up to three selected layers are concatenated. The "selected layers" column indicates the specific layers chosen for each dataset based on validation set performance. "Vanilla" refers to the embeddings extracted using the vanilla strategy, which utilizes only the 12th layer of the transformer. "S" and "P" refer to *unsupervised* embedding extraction approaches by appending a column of dummy labels with zero values and permuting each column as labels, respectively, as described in Appendix C.

| | PFN-v2 | Vanilla | S | P | layer-6 | layer-9 | layer-12 | combined | selected layers |
|---------------------------------|--------|---------|-------|-------|---------|---------|----------|----------|-----------------|
| FOREX_audchf-day-High | 77.38 | 50.68 | 56.95 | 69.48 | 68.39 | 73.57 | 74.11 | 77.11 | (5, 9, 11) |
| taiwanese_bankruptcy_prediction | 96.99 | 56.45 | 96.77 | 95.75 | 97.14 | 96.77 | 97.07 | 97.14 | (6) |
| rl | 85.51 | 50.00 | 60.56 | 70.82 | 66.90 | 69.52 | 86.72 | 87.53 | (11, 12) |
| pc3 | 89.46 | 10.22 | 89.78 | 86.90 | 90.10 | 88.82 | 88.82 | 88.82 | (8) |
| eye_movements_bin | 61.83 | 50.00 | 55.12 | 57.95 | 59.72 | 59.40 | 62.16 | 62.16 | (6, 9, 12) |
| BNG(breast-w) | 98.43 | 69.51 | 97.60 | 98.51 | 98.34 | 98.46 | 98.67 | 98.51 | (6, 9) |
| FOREX_cadjpy-hour-High | 69.53 | 51.79 | 66.55 | 71.12 | 62.12 | 64.87 | 70.66 | 70.88 | (4, 5, 6) |
| dis | 99.34 | 85.43 | 98.41 | 98.54 | 98.41 | 98.28 | 99.34 | 99.47 | (4, 5, 6) |
| sylvine | 97.46 | 85.66 | 72.78 | 95.71 | 92.49 | 93.95 | 97.27 | 96.49 | (1, 11) |
| BNG(tic-tac-toe) | 78.04 | 34.71 | 71.41 | 73.79 | 73.96 | 73.71 | 78.75 | 79.03 | (5, 10, 12) |
| online_shoppers | 90.59 | 84.51 | 85.93 | 89.46 | 90.02 | 90.11 | 90.63 | 90.02 | (8) |
| Cardiovascular-Disease-dataset | 72.84 | 50.86 | 68.73 | 72.60 | 72.96 | 73.06 | 73.14 | 73.09 | (5, 8, 12) |
| credit | 78.04 | 62.31 | 75.86 | 78.31 | 77.62 | 77.80 | 77.95 | 77.59 | (4, 6, 9) |
| FOREX_audsgd-hour-High | 67.26 | 51.48 | 65.49 | 70.14 | 57.24 | 61.06 | 69.62 | 70.41 | (7, 10, 12) |
| waveform-5000 | 86.00 | 80.60 | 55.70 | 87.10 | 85.60 | 85.60 | 86.40 | 86.90 | (1, 6, 11) |
| jungle_chess | 85.65 | 39.60 | 64.12 | 72.14 | 78.55 | 80.44 | 86.66 | 86.85 | (10, 11, 12) |
| BNG(cmc) | 57.40 | 42.62 | 52.48 | 55.16 | 56.19 | 56.72 | 57.72 | 57.88 | (9, 10, 12) |
| page-blocks | 97.35 | 94.25 | 95.43 | 96.35 | 96.07 | 96.71 | 97.17 | 97.35 | (6, 7, 12) |
| segment | 93.07 | 72.29 | 69.26 | 87.23 | 91.99 | 88.10 | 93.51 | 92.64 | (1, 12) |
| website_phishing | 90.77 | 36.90 | 82.66 | 90.04 | 85.98 | 87.08 | 91.88 | 91.88 | (7, 10) |
| baseball | 93.66 | 78.73 | 92.54 | 92.16 | 93.28 | 94.03 | 93.66 | 95.15 | (10, 11) |
| pendigits | 99.50 | 59.75 | 72.40 | 98.18 | 92.81 | 93.04 | 99.41 | 99.45 | (3, 4, 12) |
| Gender_Gap_in_Spanish_WP | 60.84 | 33.68 | 59.47 | 60.84 | 59.68 | 60.32 | 60.53 | 60.84 | (2, 12) |
| wine-quality-white | 62.35 | 10.51 | 49.29 | 55.10 | 54.08 | 55.31 | 63.57 | 64.39 | (8, 11, 12) |
| satimage | 91.21 | 82.04 | 84.99 | 89.19 | 88.72 | 88.65 | 91.91 | 91.91 | (8, 11, 12) |
| mfeat-fourier | 90.00 | 55.50 | 46.75 | 85.75 | 77.75 | 82.25 | 89.50 | 89.50 | (2, 7, 12) |
| VulNoneVul | 98.95 | 1.05 | 98.95 | 98.33 | 98.95 | 98.95 | 98.95 | 98.95 | (1) |
| law-school-admission-bianry | 100.0 | 99.83 | 79.76 | 98.82 | 100.0 | 100.0 | 100.0 | 100.0 | (6) |
| KDD | 80.34 | 78.45 | 62.36 | 76.76 | 79.34 | 78.35 | 81.23 | 79.94 | (1, 8, 10) |